UNIVERSITÀ DEGLI STUDI DI PADOVA

DIPARTIMENTO DI BIOLOGIA

Corso di Laurea in Biologia Molecolare

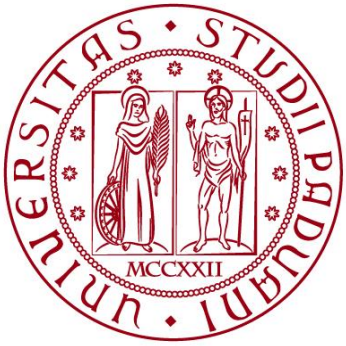

ELABORATO DI LAUREA

RUOLO DEL CANALE $K_V1.3$ E DEI SUOI MODULATORI NELLA PROGRESSIONE DELLA MALATTIA DI PARKINSON

Tutor: Prof.ssa Ildikò Szabò
Dipartimento di Biologia

Co-tutor: Michael Donadon
Dipartimento di Biologia

Laureanda: Linda Jacqueline Cattaneo

ANNO ACCADEMICO 2023/2024

Indice

Abstract

Nel presente articolo, i ricercatori sono andati a confermare con studi in vivo e in vitro il coinvolgimento della neuroinfiammazione nella progressione della malattia di Parkinson, notando un'espressione aumentata del canale potassio voltaggio-dipendente Kv1.3 nella microglia in risposta alla sua interazione con la tirosina chinasi Fyn. Questa proteina è in grado di regolare a livello post-traduzionale l'attività del canale Kv1.3 tramite fosforilazione diretta, oppure influenzarne i livelli di trascrizione: la proteina Fyn infatti attiva la chinasi PKCδ, responsabile dell'attivazione di p38 MAPK (map chinasi), la quale a sua volta contribuisce alla fosforilazione del fattore di trascrizione SP1 che agisce sul promotore del canale Kv1.3. Un'eccessiva espressione del canale viene innescata dal legame di αSyn_{AGG} (α-Sinucleina aggregata) o di LPS (lipopolisaccaride) sui PPR (Pattern Recognition Receptors) e determina l'attivazione di un profilo infiammatorio con rilascio di TNFα, IL-12, IL-1β (rispettivamente Tumor Necrosis Factor-α, Interleuchina 12 e 1β). Queste citochine secrete, portano alla morte i neuroni dopaminergici; quindi ipoteticamente se riuscisse a ridurre la loro sintesi o attivazione, si otterrebbe un recupero del fenotipo sano. A tale scopo è stato testato l'inibitore del canale, PAP-1 (5-(4-fenossibutossi) psoralene), che causa un decremento dei livelli di mRNA delle citochine e della loro attivazione ad opera del complesso proteico dell'inflammasoma NRLP3 (NOD-, LRR- and pyrin domain-containing protein 3), riducendo di conseguenza la quantità di neuroni uccisi.
Considerato il contributo del canale Kv1.3 nella neuroinfiammazione, con regolatori positivo e negativo rispettivamente Fyn e PAP-1, esso è stato ritenuto un potente marcatore diagnostico e un bersaglio terapeutico per la malattia di Parkinson.

1. Introduzione: lo scopo della ricerca

Gli autori dell'articolo hanno condotto uno studio volto a dimostrare l'implicazione della neuroinfiammazione nella progressione della malattia di Parkinson, studiando in particolare le funzioni del canale voltaggio dipendente Kv1.3 coinvolto nell'attivazione del profilo infiammatorio in cellule microgliali, in risposta ad aggregati di α-sinucleina (αSyn_{AGG}). È stato inoltre indagato il potenziale terapeutico di tale canale tramite la sua modulazione da parte della tirosina chinasi Fyn e dell'inibitore PAP-1. Dato che pazienti affetti da tale morbo mostrano un aumento dei livelli del canale Kv1.3, si ipotizza che ridurre farmacologicamente la sua attività potrebbe essere un valido trattamento per rallentare il decorso della malattia.

1.1 Morbo di Parkinson

Il morbo di Parkinson è una patologia neurodegenerativa ad evoluzione lenta, di origine multifattoriale, che consiste nella progressiva perdita funzionale e quantitativa di neuroni dopaminergici a livello della substantia nigra compatta (SNc). Questo nucleo del mesencefalo ventrale è responsabile della generazione di movimenti volontari e della modulazione di quelli involontari (1).

Tra le cause principali all'insorgenza del morbo si annoverano mutazioni a carico di 7 geni (1, 2) tra cui PARK1/4/7, SNCA e DJ-1; a cui si aggiungono traumi meccanici e fattori epigenetici, quali l'esposizione a metalli o pesticidi. Le aberrazioni genetiche sono solitamente ereditabili, autosomiche recessive, fatta eccezione per la sinucleopatia che è autosomica dominante. Quest'ultima patologia insorge quando il gene SNCA codificante l' αSyn risulta mutato; le conseguenze sono la mancanza dei meccanismi di controllo della qualità post-traduzionale delle proteine e l'aggregazione di oligomeri a livello presinaptico, che vanno ad interferire con il corretto rilascio del neurotrasmettitore dopamina. L' αSyn è una proteina fisiologicamente implicata nel trasporto vescicolare assonale, nella sintesi della dopamina e nella plasticità sinaptica; si comprende quindi come alterazioni a suo carico compromettano la capacità comunicativa dei neuroni nigrali. Quando la proteina si accumula in aggregati, è particolarmente tossica perché danneggia le membrane cellulari inclusa quella mitocondriale, alterando le loro funzioni e

generando stress ossidativo, oltre ad andare ad attivare in modo cronico la microglia, cellule del sistema immunitario presenti nel cervello. La disfunzione mitocondriale porta a ridotta produzione di ATP e aumento di ROS, che provocano danni cellulari andando ad ossidare proteine, lipidi e frammentando il DNA. A questi fattori, nei neuroni dopaminergici di pazienti affetti dal morbo, si aggiungono difetti nei meccanismi di autofagia, che riducono la capacità della cellula di eliminare gli aggregati proteici e portano al sovraccarico il sistema ubiquitina-proteasoma (2). L'αSyn è inoltre necessaria per l'omeostasi del calcio; quindi nei soggetti affetti da malattia di Parkinson (Parkinson's disease, PD) questo equilibrio fisiologico si trova alterato, innescando l'apoptosi. La combinazione stessa di questi effetti (stress ossidativo, disfunzione mitocondriale e accumulo di proteine non correttamente ripiegate) può attivare la morte cellulare programmata nei neuroni dopaminergici; di conseguenza i gangli della base in cui sono raggruppati non possono più comunicare col nucleo striato, talamo e corteccia motoria per dirigere l'avvio e la conclusione dei movimenti (1, 2). Ne risultano sintomi quali tremori, bradicinesia e appunto difficoltà nell'iniziare o terminare movimenti volontari. L'esordio della malattia si manifesta quando gran parte dei neuroni dopaminergici (all'incirca l'80%) ha perso la propria funzionalità (1).

1.2 Ruolo del canale Kv1.3 nella microglia

A contribuire alla morte neuronale entra in gioco la microglia, ossia le cellule gliali macrofagiche del sistema nervoso centrale; queste fanno parte del sistema immunitario innato che si occupa di fagocitare detriti cellulari e patogeni, ri-mielinizzare le fibre assonali danneggiate e modulare la plasticità sinaptica. Nel morbo di Parkinson la loro attivazione ha un'effetto collaterale neurotossico che porta all'incrementare della degenerazione della SNc, grazie a TLR2 (Toll-like receptor 2) che riconoscono aggregati di αSyn_{AGG}, percepiti come DAMP (Damage-associated Molecular Pattern). Tale legame porta, attraverso segnali intracellulari, alla sintesi e attivazione del fattore di trascrizione NF-kB, la cui funzione è regolare l'espressione di geni proinfiammatori IL-1β , TNFα e IL-6 (2). Affinché NF-kB possa legarsi al promotore, dev'essere scisso in un eterodimero e fosforilato dalla chinasi p38 MAP: solo in tal modo può penetrare nella membrana nucleare sotto forma di p65-p60 e svolgere la propria funzione (1, 2).

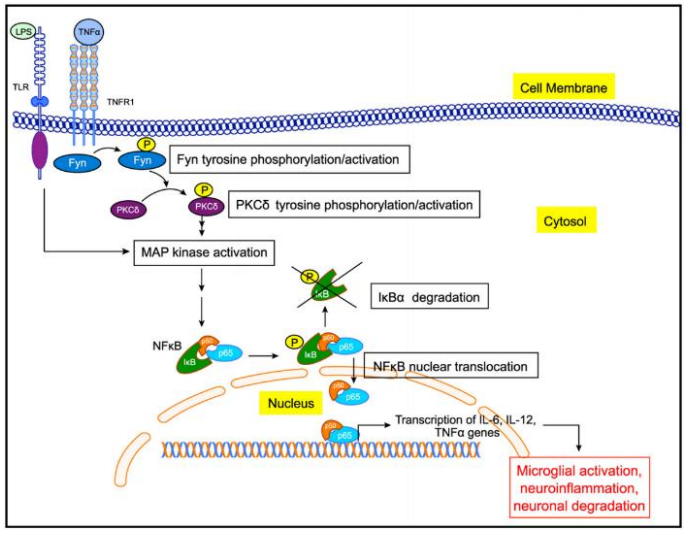

Fig. 1: Attivazione del profilo infiammatorio in microglia
Raffigura la cascata di segnalazione dalla chinasi Fyn alla dimerizzazione di NF-kB attraverso PKCδ e la chinasi MAP38
Nikhil Panicker, et al. July 8, 2015 • 35(27):10058 –10077 *The Journal of Neuroscience*

È stato scoperto che oltre alla sintesi di citochine, NF-kB incentiva anche l'espressione del canale Kv1.3 nella microglia (2), un canale voltaggio dipendente del potassio con struttura tetramerica. Ciascuno dei 4 polipeptidi α di cui è costituito il canale, presenta 1 dominio citosolico T1 e 6 segmenti transmembrana: il segmento S4 costituisce il sensore per il voltaggio e regola lo stato di apertura/chiusura del poro in dipendenza da variazioni del potenziale di membrana; mentre il segmento S6 forma le pareti del poro (3). Sono presenti siti di fosforilazione ricchi di tirosina e di serina sui quali agiscono i modulatori chinasici. Fondamentale per la funzione del canale è il filtro di selettività, rappresentato dal P-loop che si trova tra S5 e S6: esso consente il passaggio esclusivo di ioni potassio (K^+) anidri nello spazio extracellulare con flusso passivo secondo gradiente elettrochimico. Il filtro di selettività presenta la porzione strutturale maggiormente conservata dal punto di vista evolutivo (3), infatti vi sono numerose omologie con Kv1.3 in *Drosophila melanogaster* (codificato dal gene Shaker, (4)), mentre nel mammifero il gene codificante il canale è KCNA3. Tale canale è presente a livello della membrana interna dei mitocondri e nella membrana plasmatica (4). Gli autori del presente articolo si sono concentrati su quest'ultimo tipo.

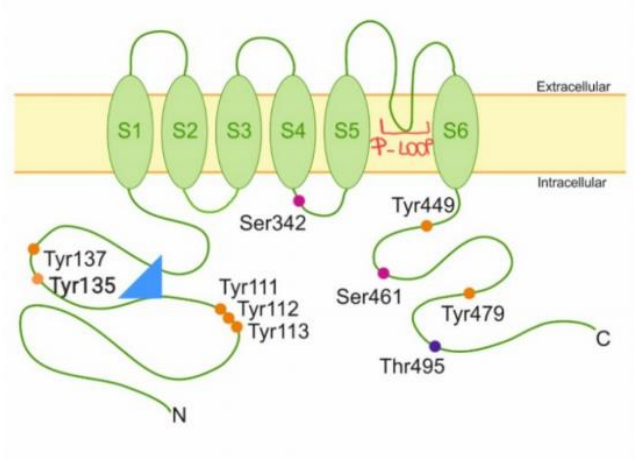

Fig. 2: Struttura del canale Kv1.3, articolato in domini citosolici N e C-terminali e segmenti transmembrana, con relativi siti di PTM
Maria Navarro-Pérez et al. 2023, 15, 2716 *Alban Girault*

Svariati motivi hanno spinto i ricercatori ad incentrare questo studio sul canale Kv1.3: nei soggetti parkinsoniani è stato riscontrato un aumento di tale polipeptide, già noto in altre patologie (5), con conseguente eccessiva secrezione di citochine, portando ad ipotizzare un suo ruolo nella neuroinfiammazione e nella morte neuronale. È stato rilevato inoltre un aumento dei livelli della tirosina chinasi Fyn, che contatta il canale nei siti ricchi di prolina tramite i suoi domini Src; si sospetta quindi un'interazione positiva tra le due componenti.

Nei casi di PD, livelli ectopici del canale Kv1.3 non sono presenti solo nella microglia, ma in tutte le cellule del sistema immunitario (anche al di fuori della barriera ematoencefalica (BBB)): infatti con saggi di qRT-PCR si rileva un suo incremento nei linfociti B e T (2, 3). Le conseguenze di questa eccessiva espressione non sono ancora completamente comprese, dal momento che il canale è implicato in molteplici fenomeni quali l'infiammazione, l'insorgenza di tumori (4), diabete (2, 5) e malattie autoimmuni. Tuttavia si comprende l'interesse nell'indagare i meccanismi molecolari della modulazione di Kv1.3 come interruttore del profilo infiammatorio nella microglia.

Attraverso studi di *knock-out* genico, il canale si è rivelato indispensabile per l'attivazione dell'inflammasoma NLRP3 (NOD-, LRR- and pyrin domain-containing protein 3). Questo complesso multiproteico si presenta tripartito tra dominio ammino-terminale PYD, centrale NACHT e carbossi-terminale LRR. Ciascuno di questi domini ha funzioni specifiche: LRR ha il compito di autoinibire

la piattaforma, NACHT è protagonista dell'assemblaggio del complesso con omoligomerizzazione; mentre su PYD si lega l'adattatore ASC che recluta la procaspasi 1, un enzima in grado di attivarsi autonomamente con taglio autoproteolitico (6). Di quest'ultima rimane legata all'inflammasoma solo la porzione cataliticamente attiva, responsabile di rendere funzionali le citochine trascritte da NF-kB. Perché si giunga all'inflammasoma attivo, tuttavia, si devono realizzare due fasi: il priming della cellula con DAMP/PAMP e l'attivazione della complesso proteico (6). Il match con fattori esogeni o di danno (come LPS, αSyn_{AGG}, citochine profiammatorie o mtROS) serve per indurre la trascrizione dell'inflammasoma NLRP3 e della caspasi 1, nonché a stabilizzare il complesso multiproteico con modificazioni post-traduzionali (6). La seconda fase consiste nell'attivazione vera e propria di NLRP3: la piattaforma si assembla per oligomerizzazione del monomero PYD-NACHT-LRR, scatenata dall'efflusso di K^+ (Fig. 3). Essendo l'inflammasoma adibito all'attivazione delle citochine si riscontra una ridotta secrezione di TNFα, IL-1β e IL-12 quando si va a silenziare il canale.

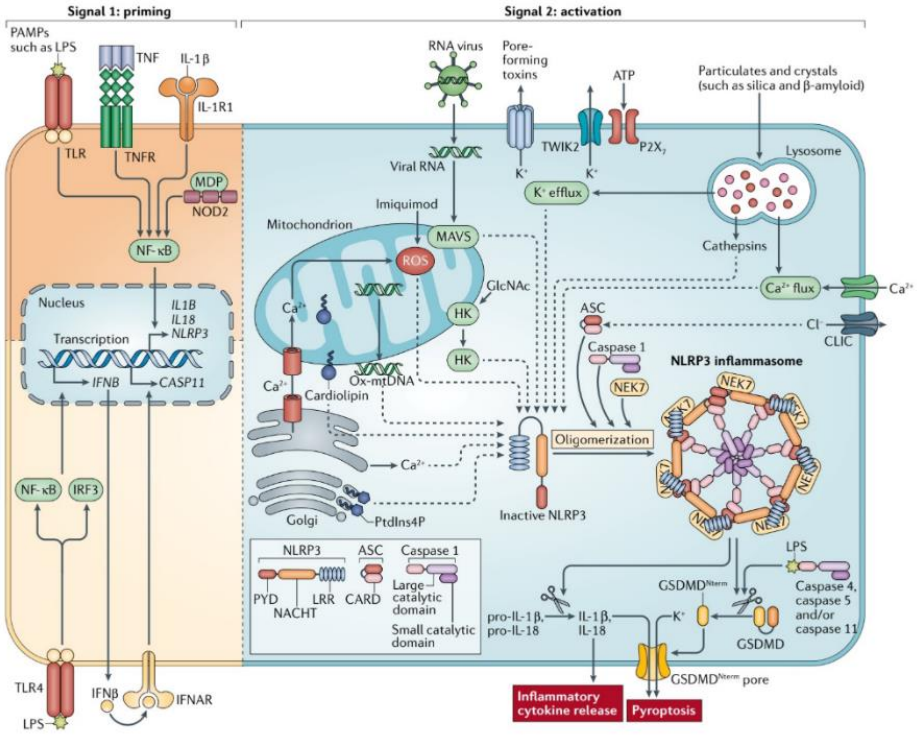

Fig. 3: Meccanismi di priming e attivazione di NLRP3
I processi intracellulari sono dipendenti gli uni dagli altri a cascata
Karen V. Swanson, et al. August 2019 *Nature Reviews*

Si comprende quindi esserci una sinergia tra le citochine prodotte da NF-kB in conseguenza al legame di αSyn_{AGG} ai PRR (Pattern Recognition Receptors) e l'assemblaggio dell'inflammasoma funzionante, che rende attive le molecole infiammatorie e le rilascia in forma solubile nella matrice extracellulare. Qui le citochine vanno a favorire l'eliminazione delle cellule danneggiate a cui si legano tramite i rispettivi recettori; il tutto in aggiunta alla fagocitosi già messa in atto da parte della microglia.

1.3 Induzione e risoluzione della malattia in laboratorio

Per studiare *in vivo* il morbo di Parkinson in laboratorio si impiega l'organismo *Mus musculus*, tuttavia, considerata l'origine multifattoriale della malattia, non esiste un unico sistema per riprodurre *in vivo* tutte le cause eziologiche; quindi si procede con lo studio su più modelli in parallelo. Nell'articolo che viene presentato ne vengono assunti principalmente tre: il MitoPark, dove i neuroni dopaminergici presentano il fattore di trascrizione mitocondriale A (TFAM) inattivato; Syn–adeno-associated virus (αSyn-AAV), in cui si induce la malattia mediante trasfezione di un vettore virale contenente il gene per l' αSyn; ed infine il modello con MPTP (1-metil 4-fenil 1,2,3,6-tetraidro-piridina) che causa disfunzioni mitocondriali senza accumuli proteici. La morte mirata dei neuroni dopaminergici da parte del MPTP simula i sintomi osservati nel PD, come la perdita di controllo motorio e le disfunzioni cognitive, in quanto questa neurotossina induce un lento decorso alla patologia con riduzione della massa della SNc.

Successivamente per ciascun modello murino sono stati quantificati i livelli trascrizionali e proteici del canale Kv1.3, rilevando elevate quantità di tale proteina, così come nei campioni postmortem di umani affetti da PD. In tutti e tre i modelli utilizzati, si sono ottenuti risultati consistenti tra loro: dalla qRT-PCR sono risultati maggiori livelli di mRNA in campioni affetti rispetto ai controlli, dal Western Blot si è evidenziata la presenza di elevate concentrazioni proteiche di Kv1.3 oltre che di αSyn_{AGG} (eccetto che nel modello con MPTP) e con misurazioni della corrente (tramite *patch clamp*) attraverso Kv1.3 si è capito che le proteine altamente espresse corrispondono a canali Kv1.3 attivi.

La morte dei neuroni dopaminergici, di conseguenza, innesca un loop che porta ad un'ulteriore degenerazione, in quanto il contatto della microglia con gli aggregati

di αSyn_{AGG} (o in caso di infezione con LPS) porta ad un aumento dell'espressione del canale e all'attivazione della microglia in uno stato pro-infiammatorio con rilascio di citochine attive. Questo scatena un'infiammazione cronica e l'ulteriore degenerazione dei neuroni dopaminergici. Dato il coinvolgimento del canale Kv1.3 nell'attivazione della microglia, è stato ipotizzato che l'inibizione del canale possa ridurre lo stato infiammatorio e favorire un rallentamento nella progressione della malattia. Un efficace inibitore testato a tale scopo è PAP-1 (5-(4-fenossibutossi) psoralene), una molecola permeabile alla barriera ematoencefalica (BBB) e quindi somministrabile farmacologicamente in modo non invasivo. Per anni la difficoltà è stata trovare un inibitore che fosse specifico per questo canale e non interferisse con l'attività di canali simili. I punti di forza di PAP-1 sono proprio la specificità ed l'elevata affinità per Kv1.3: agisce infatti come un competitor al flusso cationico legandosi al segmento S6 che forma il poro del canale. Si inserisce preferibilmente nello stato aperto del canale (9), riducendone l'attività come verificato tramite *patch clamp*. Non potendosi legare ad altri canali del K^+ oltre che al Kv1.3, diventa uno strumento utile per studiare ulteriori funzioni di tale canale nelle cellule immunitarie. Gli autori hanno iniziato quindi a testare il valore terapeutico di PAP-1 per la cura di tale morbo tramite l'utilizzo di modelli Mitopark e MPTP con risultati coerenti con quanto atteso. Il recupero del fenotipo è stato valutato con test di moto-coordinazione; mentre con analisi biochimiche sono stati misurati i livelli della dopamina; infine è stato verificato lo stato pro-infiammatorio o anti-infiammatorio della microglia analizzando la sua morfologia. Tutte queste analisi hanno dato risultati molto promettenti. L'inibitore è stato testato principalmente su modelli animali quali ratto e topo, ed attualmente si valuta la possibilità di trattamenti su campioni umani, non solo per il trattamento del PD ma anche in casi di malattie autoimmuni, aterosclerosi e diabete (4, 5), malattie che presentano uno stato infiammatorio cronico.

2. Materiali e metodi

2.1 Western Blot

La tecnica prevede l'omogenizzazione di cellule o tessuto con buffer RIPA per l'estrazione di proteine che poi sono state quantificate tramite Bradford e normalizzate nella loro concentrazione per assicurarsi di caricarne eguali quantità tra i diversi campioni (30-40 µg). Si procede con la separazione delle proteine sulla base del peso molecolare con SDS-page, una corsa elettroforetica denaturante in cui l'SDS carica negativamente tutte le biomolecole in analisi, cosicché possano separarsi secondo dimensione e non proprietà biochimiche. La matrice di poliacrilammide utilizzata è concentrata al 10-18% e la corsa procede a 4°C, 110 V per 2-3 ore. In seguito si esegue il trasferimento delle proteine separate su supporto di nitrocellulosa (blot), passaggio necessario per rendere le molecole accessibili agli anticorpi che verranno utilizzati in seguito; le porzioni di membrana che non hanno legato bande vengono bloccate con buffer LI-COR per 1 h per prevenire legami aspecifici. Sono stati utilizzati anticorpi primari anti-Kv1.3, anti-p38, anti-PKCδ e anti-NLRP3. A ognuno di questi anticorpi (incubati overnight a 4°C) se ne coniuga uno secondario anti-mouse o rabbit (a seconda della specie in cui è stato prodotto l'anticorpo primario) che permette di visualizzare al transilluminatore le bande proteiche legate dal primario sfruttando il principio della chemioluminescenza. Per controllare il caricamento di ogni campione sono stati utilizzati anticorpi primari anti-β-actina e anti-tubulina. Tra un'incubazione e la successiva è importante rimuovere l'eccesso di anticorpo non legato con 7 lavaggi in PBS1X°+Tween 0,05%.

2.2 qRT-PCR

Per misurare l'espressione genica in diverse condizioni si parte dall'estrazione dell'RNA totale con TRIZOL, per poi retrotrascrivere 1 µg di RNA con il kit "High Capacity cDNA Synthesis". Per sapere quale volume prelevare per avere 1 µg di RNA, viene quantificata la concentrazione dei campioni con il NanoDrop. La retrotrascrizione da RNA a cDNA è necessaria perché la Taq polimerasi riconosce unicamente quest'ultimo come substrato da amplificare. La master mix di qRT-PCR impiegata è RT2 SYBR Green a cui vengono aggiunti primers complementari

a specifici trascritti d'interesse. Questa tecnica è permette di verificare i livelli di mRNA presente nei campioni tramite le curve d'amplificazione; infatti a partire dal ciclo soglia al quale la fluorescenza emessa diventa visibile, è possibile dedurre la quantità di trascritti che erano inizialmente presenti nel campione, ossia i livelli di espressione genica.
Nel presente studio il saggio è stato utilizzato per valutare i livelli di trascritti di Kv1.3, TNFα, pro-IL-1β e la chinasi Fyn, mentre come controllo si è utilizzato il gene housekeeping 18S rRNA.

2.3 Whole-cell patch clamp

Saggio di elettrofisiologia impiegato per misurare l'attività del canale Kv1.3 in configurazione whole-cell. Le cellule microgliali primordiali (PMCs) vengono piastrate con una distribuzione di 100,000-150,000 cellule in 24 pozzetti per 8-12 ore prima di stimolarle con 300 ng/mL di LPS o αSyn_{AGG}. In seguito vengono distaccate con tripsina, lavate e ancorate ad un vetrino di poli-L-lisina. In tale configurazione una porzione di membrana delle cellule viene risucchiata con la pipetta e strappata facendo trazione, così da accedere al citosol e poter misurare la corrente totale tramite un amplificatore EPC-10 HEKA. La soluzione interna alla pipetta contiene : [KF]= 145mM, [$MgCl_2$]= 2mM, [HEPES]= 10mM, [EGTA]= 10mM, ed è priva di Ca^{2+} così da evitare la contaminazione delle correnti di K^+ con canali attivati da calcio. Mantenendo il voltaggio costante a +40 mV, si misura in condizioni diverse quale sia la corrente necessaria a mantenere tale differenza di potenziale ai capi della membrana. In tal modo si è andati a rilevare l'attività del canale in linfociti di pazienti affetti da PD, risultata aumentata rispetto i controlli sani così come in PMCs (primary microglial cells) di modelli murini parkinsoniani. Hanno sfruttato questa tecnica anche per studiare la funzione della tirosina chinasi Fyn dopo averne eseguito *knock-out* oppure inibizione con saracatinib (1 μM); così come le funzioni di PKCδ e PAP-1 in relazione al canale d'interesse sono state studiate in tal modo.

2.4 IHC e ICC

L'immunocitochimica (ICC) è una tecnica che utilizza anticorpi specifici per rilevare e visualizzare la localizzazione subcellulare di proteine specifiche

all'interno di singole cellule isolate; l'immunoistochimica (IHC) invece si applica a sezioni encefaliche di 30 μm e quindi rileva la distribuzione proteica a livello tissutale. In entrambi i saggi, gli studi sono condotti ex vivo. Per quanto riguarda la ICC, dopo il fissaggio delle cellule in paraformaldeide al 4%, si esegue un'*antigen retrieval* per smascherare gli epitopi potenzialmente oscurati durante l'ancoraggio e renderli facilmente accessibili agli anticorpi. Quindi le cellule vengono lavate in PBS, segue il buffer di blocco e un'incubazione overnight a 4°C con l'anticorpo primario. Si ripete il lavaggio in PBS, poi l'incubazione con anticorpo secondario coniugato a Alexa-dye. I vetrini vengono analizzati al microscopio confocale a fluorescenza. La IHC prevede un protocollo analogo, con la differenza che i campioni vengono colorati con colorante nucleare Hoechst e visualizzati al microscopio a fluorescenza invertito.

2.5 Modelli: in vivo

- MitoPark: topo transgenico che sviluppa una progressiva neurodegenerazione dopaminergica, utilizzato per convalidare il potenziale terapeutico di PAP-1. È un modello assunto per riprodurre le disfunzioni mitocondriali caratteristiche del PD; inoltre porta ad un aumento dei trascritti del canale d'interesse.
- MPTP: modello di PD subacuto, ottenuto iniettando 20 mg/kg al giorno per 4 giorni consecutivi e sacrificati al quinto. Genera disfunzioni mitocondriali che portano alla morte del neurone senza aggregati di αSyn.
- αSyn-AAV: l'aggregazione di αSyn viene indotta mediante trasfezione di un vettore virale codificante il suo gene.

Modelli: ex vivo

- PMCs: *primary microglial cells*, cellule microgliali estratte dalla substantia nigra compatta, non ancora andate incontro a divisione mitotica; su di esse sono stati condotti la maggior parte dei saggi, in particolare di elettrofisiologia.

3. Risultati

3.1 Kv1.3 è l'interruttore per la morte neuronale

Il coinvolgimento della microglia nella malattia di Parkinson era già noto 30 anni fa (1), grazie al presente studio è stato possibile definire in modo più approfondito il meccanismo molecolare col quale si realizza: la scoperta dell'aumentata espressione del canale Kv1.3 ha spinto i ricercatori a studiarne le funzioni, rivelando così che funge da interruttore per il rilascio di citochine attive. Queste molecole hanno poi l'effetto collaterale di uccidere i neuroni circostanti contribuendo alla neurodegenerazione parkinsoniana. Ciò spiega perché il canale Kv1.3 sia così importante nei soggetti affetti da PD e nei modelli murini: l'incremento di espressione si presenta sia a livello trascrizionale, rilevato con saggi di qRT-PCR, che a livello funzionale, mostrato con misurazioni di corrente in *patch clamp*. Infatti in presenza di aggregati si registra un incremento del flusso attraverso questo tipo di canale, come mostrato in Fig. 4.

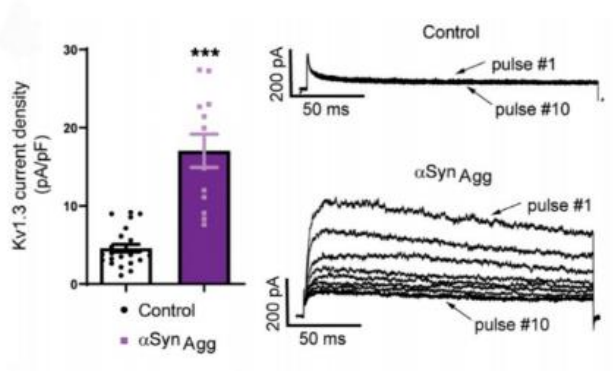

Fig. 4: Registrazione whole-cell *patch clamp* di PMCs trattate con αSynAGG (1 µM) per 24-48 h
Si osserva un incremento dell'attività di canale Kv1.3 nei campioni trattati

3.2 Gli aggregati di α-Sinucleina attivano cronicamente il profilo infiammatorio in microglia

Un requisito necessario per l'attivazione della microglia, come accennato precedentemente, è il legame di LPS o αSyn_{AGG}, a cui consegue un aumento nella trascrizione di Kv1.3, come osservato in campioni umani postmortem e in modelli MitoPark di 16-24 settimane. Nel campione di controllo dove la microglia non è sovra-attivata, il canale presenta livelli fisiologici di mRNA, come mostrato dalla qRT-PCR in Fig. 5; mentre aumentano del doppio in

presenza di LPS, infine tendono a diminuire in risposta a IL-4. Tra i vari pathways di attivazione possibili, quello osservato nella microglia con gli esperimenti è di tipo classico, ossia indotto da fattori esogeni che portano il soma ad ingrandirsi e ridurne il numero di bracci.

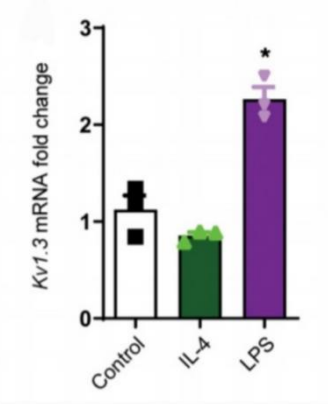

Fig. 5: Livelli dei trascritti di Kv1.3 in condizioni fisiologiche, anti-infiammatorie con IL-4 (20 ng/mL) ed infiammatorie con LPS (1 µg/mL)

3.3 Kv1.3 è specificatamente e altamente espresso dalla microglia di modelli PD

Un aspetto interessante è l'aumentata espressione che si manifesta specificatamente a carico del canale Kv1.3, non in altri tipi di canali K^+ voltaggio-dipendenti né in generale a livello di proteine totali nelle cellule; infatti nel Western blot (Fig. 6) si può osservare la banda inalterata del controllo di β-actina, mentre quella del canale è di intensità maggiore in presenza di aggregati. Poiché tale aumento di espressione si manifesta in MMCs (cellule microgliali murine) stimolate con LPS o αSyn_{AGG}, ciò fa supporre che il canale sia coinvolto nell'attivazione del profilo infiammatorio e quindi abbia una responsabilità nella patogenesi e progressione del Parkinson.

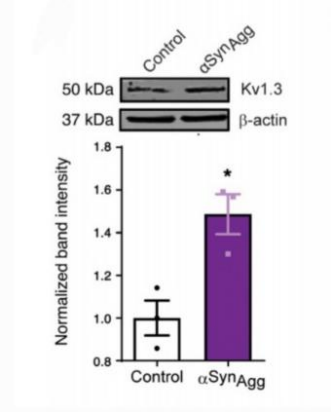

Fig. 6: Western blot dei livelli proteici di Kv1.3 indotti da αSyn_{AGG} (1 µM) per 24-48 h in MMCs
Si osserva un aumento di espressione del canale in presenza di aggregati proteici

3.4 Kv1.3 è un potenziale marcatore diagnostico

Per stabilire ulteriormente la rilevanza clinica del canale in PD, gli autori ne hanno analizzato i livelli d'espressione in cervelli umani parkinsoniani postmortem ed hanno riscontrato significativi aumenti nelle fasi precoci della malattia piuttosto che negli stadi tardivi (Fig. 7); questa evidenza apre la possibilità di utilizzare il canale come biomarcatore diagnostico. Inoltre, il potenziamento del canale non si limita alle cellule gliali ma a tutte le cellule del sistema immunitario (2, 3), conferendo ulteriore importanza all'analisi della sua espressione.

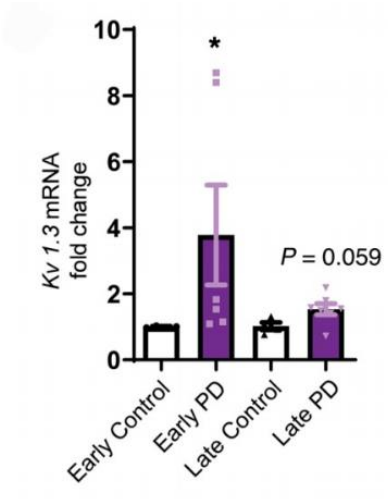

Fig. 7: Quantità di trascritti di Kv1.3 nel decorso della patologia

3.5 La chinasi Fyn modula la trascrizione di Kv1.3 nella microglia tramite l'asse Fyn/PKCδ

Dopo aver attestato livelli ectopici del canale dal punto di vista proteico e funzionale, gli autori dell'articolo sono andati a verificare quale fosse il meccanismo molecolare responsabile di tali incrementi: hanno scoperto che il promotore di Kv1.3 presenta molteplici siti di legame per i fattori di trascrizione NF-kB e Sp1. È stato riscontrato che Sp1 viene fosforilato dalla chinasi p38 MAP, a monte del quale agisce la chinasi Fyn: questa infatti è in grado di attivare la chinasi proinfiammatoria e proapoptotica PKCδ , che a sua volta attiva p38 MAPK; ma poiché p38 MAPK permette la fosforilazione del fattore di trascrizione SP1 che agisce sul promotore di Kv1.3, allora l'asse Fyn/PKCδ modula la trascrizione del canale. Questa deduzione viene sostenuta dalla quantificazione dei trascritti di Kv1.3: notiamo che il canale è sovra-espresso nei casi con tirosina chinasi funzionante; mentre dove viene fatto *knock-out* o inibizione della Fyn con

saracatinib (1μM), il canale perde di espressione (Fig. 8) e di attività (rilevati rispettivamente con Qrt-pcr e *patch clamp* in PMCs). I controlli sono coerentemente uguali tra loro.

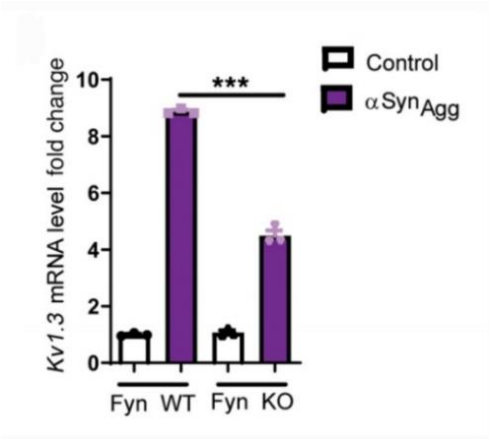

Fig. 8: qRT-PCR del canale in condizioni di chinasi Fyn wildtype o *knock-out*, riporta una maggiore induzione all'espressione del canale in presenza dell'enzima WT

3.6 Il fattore di trascrizione NF-kB è necessario per sovra-esprimere il canale Kv1.3

Per verificare ulteriormente le funzioni di p38 MAPK e NF-kB come fattori di trascrizione, le cellule sono state trattate con i rispettivi inibitori ottenendo un'attenuazione della sovra-espressione del canale (2), confermando l'ipotesi.
In sintesi perché l'espressione di Kv1.3 aumenti sono necessari αSyn_{AGG} o LPS, NF-kB e p38 MAPK, con quest'ultimi due attivati indirettamente dalla chinasi Fyn che funge da regolatore a monte della trascrizione del canale.

3.7 La chinasi Fyn modula il canale mediante fosforilazione

Approfondendo poi le funzioni della chinasi Fyn, si è scoperto essa regoli, oltre che indirettamente i livelli di trascrizione del canale Kv1.3, anche direttamente la sua attività con fosforilazione post-traduzionale. In particolare essa è in grado di legarsi con la porzione Src ai domini ricchi di prolina sull'estremità amminica del canale, per fosforilare il residuo di tirosina in posizione 135. Questo amminoacido assume rilevanza perché dal multi-allineamento col software T-Coffee risulta essere conservato in tutte le specie (2). Andando infatti a variare la tirosina in alanina mediante trasfezione di un plasmide codificante per il canale mutato, diminuisce la

PTM (post-translational modification, Fig. 9) ed i livelli di mRNA dei fattori pro-infiammatori. Infine si è verificato che la chinasi Fyn fosforilando il canale incrementa la funzione dell' αSyn_{AGG} nell'attivare Kv1.3, infatti nei casi di *knock-out* dell'enzima si ottiene un'attenuazione di tale stimolazione. Ciò viene dimostrato con registrazioni dell'attività del canale con *patch clamp*, dove le PMCs $Fyn^{-/-}$ trattate con αSyn_{AGG} o LPS mostrano livelli di corrente inferiore alle cellule $Fyn^{+/+}$ (Fig. 10).

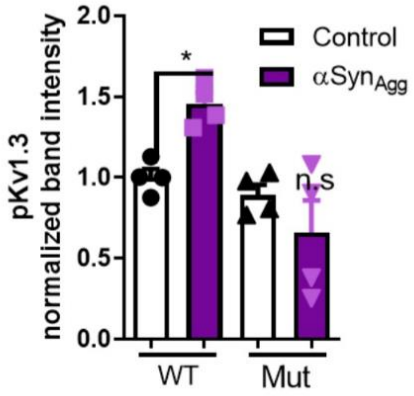

Fig. 9: Western blot che mostra come l' αSyn_{AGG} induce la fosforilazione del canale Kv1.3 WT ma non di quello mutato, in cellule microgliali murine rese immortali (MMCs)

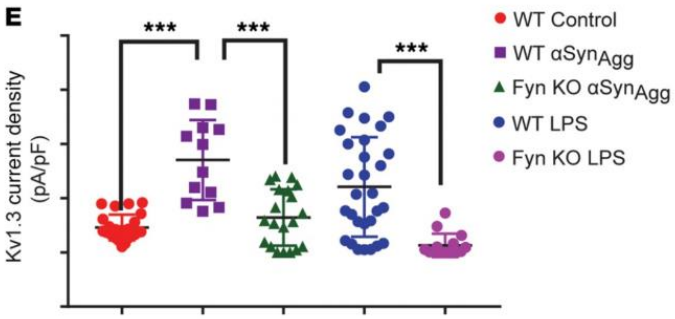

Fig. 10: Registrazione di corrente con whole-cell patch clamp illustrante un'attenuazione dell'induzione all'espressione di Kv1.3 da parte di αSyn_{AGG} o LPS quando la chinasi Fyn è assente.

3.8 PAP-1 riduce la neuroinfiammazione in modelli di PD

Il secondo grande punto di indagine degli autori è stata la funzione della molecola solubile PAP-1: quando viene co-iniettata all'MPTP, si verifica una riduzione di microgliosi (Fig. 11) e dei livelli di trascritti di Nos2, IL-6, TNFα e pro-IL-1β; nonché un calo nella perdita di neuroni nella SNc (identificabile marcando nelle cellule la tirosina idrossilasi TH, un enzima che catalizza la prima reazione della

biosintesi delle catecolamine). Anche la morfologia della microglia in presenza dell'inibitore è coerente con il mantenimento di un profilo anti-infiammatorio: sono presenti numerosi prolungamenti citoplasmatici e il soma è piccolo (Fig. 11).

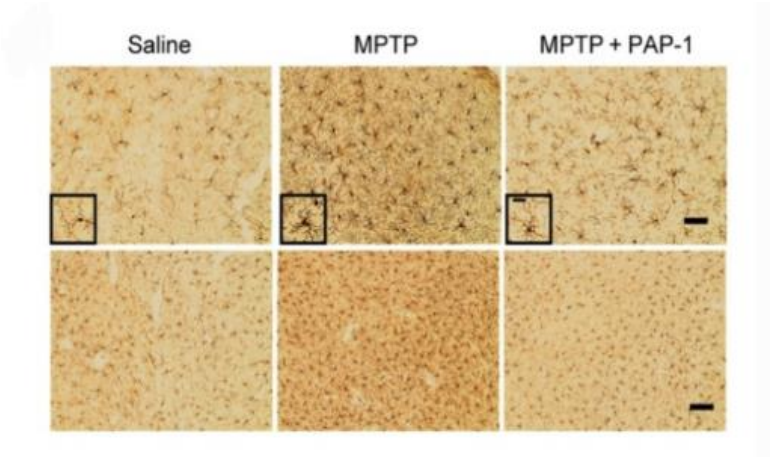

Fig. 11: Sezioni IHC con IBA-1 della SNc, scala 50-100 um.
Indicano che PAP-1 inibisce la morfologia infiammatoria

La funzione inibitrice di PAP-1 sul canale Kv1.3 viene ulteriormente accertata attraverso registrazioni whole-cell in *patch clamp* dove si osserva una notevole diminuzione del flusso cationico attraverso il canale (Fig. 12).

In tal senso PAP-1 si può configurare come un potenziale strumento terapeutico: bloccando l'attività di Kv1.3 (che rappresenta un segnale a monte essenziale all'attivazione dell'inflammasoma NRLP3) si attenuano significativamente i livelli di mRNA dei fattori proinfiammatori, l'espressione del complesso multiproteico e la secrezione delle citochine tradotte.

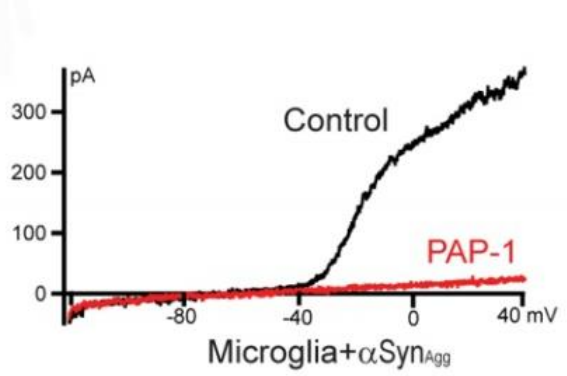

Fig. 12: Corrente attraverso Kv1.3 rilevata in presenza di PAP-1 (1 μM)
con *patch clamp* da -120 mV a +40mV

3.9 Il potenziale clinico di PAP-1 nel ristabilire la massa nigrale, le abilità motorie ed i livelli di dopamina

I saggi comportamentali post-iniezione di PAP-1 nei modelli Mitopark e MPTP-induced Parkinson rivelano una notevole riduzione dei deficit motori, testati col Rotarod (sistema rotante che valuta la coordinazione motoria, necessaria per rimanere sulla rotella per un tempo prestabilito senza cadere). Il potenziale clinico di PAP-1 è stato vagliato anche con analisi biochimiche del livello di dopamina rilasciata dai neuroni, che è tornata a valori prossimi a quelli WT; quindi PAP-1 protegge i neuroni dalla morte in contesto infiammatorio. Inoltre PAP-1 si presta a ridurre la perdita neuronale (identificata con IHC su TH) sia nel modello progressivo di Parkinson (MitoPark), sia quando la patologia viene indotta con MPTP; di conseguenza si evidenzia un recupero della massa nigrale in sezione (Fig. 13).

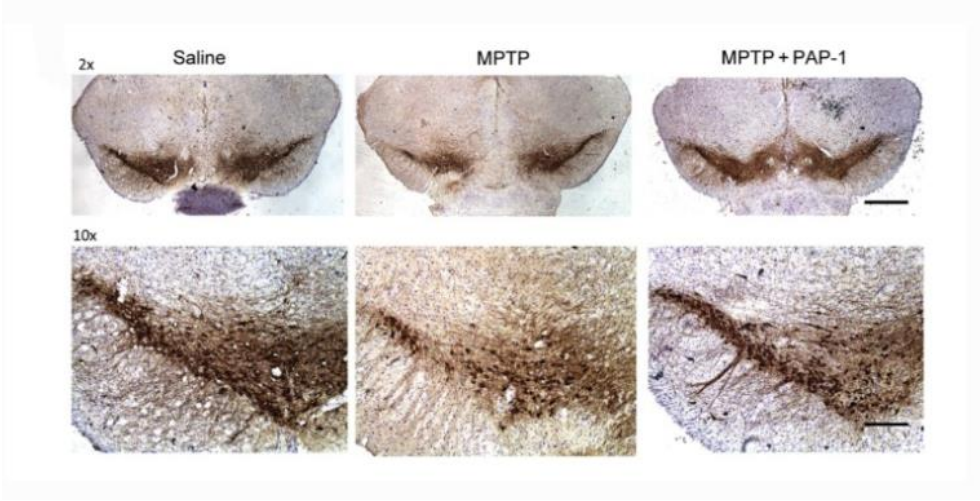

Fig. 13: Sezioni IHC su TH della SNc, scala 50-100 um
Mostrano un calo nella perdita di neuroni nella SNc trattata con MPTP e PAP-1

Tutte queste evidenze permettono di capire che il canale è altamente indotto in campioni umani e murini affetti da PD e che può fungere da target per l'immunosoppressione, nonché per la diagnosi precoce della malattia.

4. Discussione e conclusioni

L'importanza di tale articolo si configura nell'essere la prima evidenza sperimentale che il canale Kv1.3 sia sovra-espresso nella microglia di soggetti parkinsoniani, in dipendenza dall'asse Fyn/PKCδ come risposta a stimoli infiammatori. L'approccio multi-prospettico assunto dai ricercatori, volto a comprovare i risultati ottenuti testando modelli differenti di PD e valutando sia i livelli di trascritti che proteici del canale, dei modulatori e dei prodotti infiammatori, ha senz'altro dato credibilità all'articolo. Se avessero utilizzato un solo modello murino per simulare il morbo avrebbero infatti lasciato spazio al dubbio che i risultati ottenuti fossero strettamente dipendenti dalle condizioni sperimentali con cui si era indotta la malattia; invece utilizzando 3 modelli distinti per riprodurre in laboratorio questa patologia multifattoriale e confrontando al contempo i risultati con campioni umani postmortem, hanno dimostrato la consistenza e veridicità delle loro scoperte.

Tuttavia resta da verificare con ulteriori accertamenti il ruolo della chinasi Fyn nella regolazione post-traduzionale del canale, perché come riportato dagli autori, la trasformazione di microglia con mutanti di Kv1.3 sulla tirosina 135 hanno rivelato solo una modesta riduzione dell'infiammazione, lasciando sottintendere che potrebbero essere implicati altri fattori intermedi. Infatti sul canale sono presenti siti di fosforilazione per numerose chinasi: ad esempio la PKC, che ne determina l'inattivazione aggiungendo gruppi fosfato all'estremità C, oppure la chinasi MAPK che regola lo stato di apertura di Kv1.3 incentivandolo (9). Si intuisce esserci una gerarchia di PTM che in futuro dovrà essere chiarita per avere piena comprensione della regolazione del canale, che ricordo essere implicato nella divisione cellulare, apoptosi e proliferazione (9); quindi ha effetti a largo spettro sulle cellule del sistema immunitario. Inoltre, la scoperta del presente articolo riguardante l'aumento dell'attività del canale in conseguenza alla fosforilazione della tirosina 135, non trova riscontro in letteratura (9) dove anzi si riporta che le fosforilazioni su serina o tirosina vanno piuttosto ad inibire il target; quindi andrebbero fatti approfondimenti per giustificare tale discrepanza.

Volendo ricercare un altro punto debole di questo lavoro scientifico accennerei alla mancanza di corrispondenza tra i livelli di mRNA e proteine di Kv1.3, lasciato

inspiegato dagli autori, ma probabilmente dovuto a differenti sensibilità dei saggi con cui sono stati rilevati (qRT-PCR ha un potere di risoluzione maggiore) oppure alla presenza di processi post-trascrizionali intermedi non ancora noti. Per esempio gli autori stessi accennano ad un'interazione tra Fyn e AP-1, un adattatore proteico necessario per la formazione di vescicole che trasportano il canale dall'apparato del Golgi alla membrana; questa proteina potrebbe essere un ulteriore punto di regolazione per l'espressione del canale.

Ritornando al caso in studio e per concludere, la fosforilazione ad opera della chinasi Fyn rappresenta un buon meccanismo di regolazione dell'espressione genica perché è una PTM reversibile con fosfatasi, quindi approfondire tale enzima è stata una buona scelta da parte dei ricercatori per futuri trattamenti terapeutici. I modulatori di Kv1.3 ed il canale stesso infatti, considerate le evidenze sperimentali, danno la speranza di sfruttarli come biomarcatori diagnostici e immunosoppressori al fine di rallentare la progressione della malattia di Parkinson.

5. Bibliografia

1) Eric Kandel, et al. Principi di neuroscienze *Casa editrice Ambrosiana* 2023 pagine 884-890
2) Souvarish Sarkar, et al. Kv1.3 modulates neuroinflammation and neurodegeneration in Parkinson's disease *J Clin Invest*. 2020;130(8):4195-4212
3) Purushotham Selvakumar, et al. Structures of the T cell potassium channel Kv1.3 with immunoglobulin modulators, Purushotham Selvakumar *Nature Communications* | (2022) 13:3854
4) Andrzej Teisseyre, et al. Voltage-Gated Potassium Channels Kv1.3, potentially New Molecular Target in Cancer Diagnostics and Therapy* *Adv Clin Exp Med* 2015, 24, 3, 517–524
5) Julián Zayas-Arrabal, et al. Kv1.3 Channel Blockade Improves Infammatory Profile, Reduces Cardiac Electrical Remodeling, and Prevents Arrhythmia in Type 2 Diabetic Rats *Cardiovascular Drugs and Therapy* (2023) 37:63–73
6) Karen V. Swanson, et al. The NLRP3 inflammasome: molecular activation and regulation to therapeutics *Nature Reviews Immunology* August 2019 pages 477-489 (2019)
7) Nikhil Panicker, et al. Fyn Kinase Regulates Microglial Neuroinflammator Responses in Cell Culture and Animal Models of Parkinson's Disease *The Journal of Neuroscience*, July 8, 2015 • 35(27):10058 –10077
8) Meccanismi di vulnerabilità dei neuroni dopaminergici mesencefalici di ratto esposti a fattori neurotossici ambientali (di Maria Letizia Cucchiaroni, Università degli Studi di Roma Tor Vergata 2008/2009)
9) Maria Navarro-Pérez et al. The Phosphorylation of Kv1.3: A Modulatory Mechanism for a Multifunctional Ion Channel *Alban Girault* 2023, 15, 2716.

Kv1.3 modulates neuroinflammation and neurodegeneration in Parkinson's disease

Souvarish Sarkar,[1] Hai M. Nguyen,[2] Emir Malovic,[1] Jie Luo,[1] Monica Langley,[1] Bharathi N. Palanisamy,[1] Neeraj Singh,[1] Sireesha Manne,[1] Matthew Neal,[1] Michelle Gabrielle,[3] Ahmed Abdalla,[1] Poojya Anantharam,[4] Dharmin Rokad,[1] Nikhil Panicker,[1] Vikrant Singh,[2] Muhammet Ay,[1] Adhithiya Charli,[1] Dilshan Harischandra,[1] Lee-Way Jin,[5] Huajun Jin,[1] Srikant Rangaraju,[6] Vellareddy Anantharam,[1] Heike Wulff,[2] and Anumantha G. Kanthasamy[1]

[1]Parkinson Disorders Research Laboratory, Department of Biomedical Sciences, Iowa State University (ISU), Ames, Iowa, USA. [2]Department of Pharmacology, School of Medicine, UCD, Davis, California, USA. [3]Department of Biochemistry, University of Western Ontario, London, Ontario, Canada. [4]Department of Veterinary Diagnostic and Production Animal Medicine, Veterinary Medicine Building, ISU, Ames, Iowa, USA. [5]M.I.N.D. Institute, Alzheimer's Disease Center, Department of Pathology and Laboratory Medicine, UCD, Davis, California, USA. [6]Department of Neurology, Emory University School of Medicine, Atlanta, Georgia, USA.

Characterization of the key cellular targets contributing to sustained microglial activation in neurodegenerative diseases, including Parkinson's disease (PD), and optimal modulation of these targets can provide potential treatments to halt disease progression. Here, we demonstrated that microglial Kv1.3, a voltage-gated potassium channel, was transcriptionally upregulated in response to aggregated α-synuclein (αSyn_{Agg}) stimulation in primary microglial cultures and animal models of PD, as well as in postmortem human PD brains. Patch-clamp electrophysiological studies confirmed that the observed Kv1.3 upregulation translated to increased Kv1.3 channel activity. The kinase Fyn, a risk factor for PD, modulated transcriptional upregulation and posttranslational modification of microglial Kv1.3. Multiple state-of-the-art analyses, including Duolink proximity ligation assay imaging, revealed that Fyn directly bound to Kv1.3 and posttranslationally modified its channel activity. Furthermore, we demonstrated the functional relevance of Kv1.3 in augmenting the neuroinflammatory response by using Kv1.3-KO primary microglia and the Kv1.3-specific small-molecule inhibitor PAP-1, thus highlighting the importance of Kv1.3 in neuroinflammation. Administration of PAP-1 significantly inhibited neurodegeneration and neuroinflammation in multiple animal models of PD. Collectively, our results imply that Fyn-dependent regulation of Kv1.3 channels plays an obligatory role in accentuating the neuroinflammatory response in PD and identify Kv1.3 as a potential therapeutic target for PD.

Introduction

Parkinson's disease (PD) is a complex neurodegenerative disorder that is characterized mainly by the slow and progressive loss of dopaminergic neurons in the substantia nigra pars compacta (SNpc) region of the brain. This progressive loss of neurons is also associated with the release of a misfolded and aggregated protein, α-synuclein (αSyn), which is predominantly expressed in neurons throughout the brain. Recent studies have further shown the loss of extrastriatal neurons and the presence of nonmotor deficits in PD (1, 2). Though the underlying cause of this neuronal loss is not completely understood, postmortem studies have implicated nigral inflammation characterized by persistent and excessive microgliosis and astrogliosis in the pathophysiology of PD. The hypothesis that neuroinflammation is critical to PD progression is further supported by evidence from cell cultures, animal models, and postmortem human tissue analysis (3–6). Currently, there are no treatments to prevent the progression of PD, and the only available therapies are directed toward mitigating its symptoms.

Gene mutations (e.g., *PARK1/4*) can lead to misfolding and aggregation of αSyn, the accumulation of which into Lewy bodies and neurites is the hallmark of both sporadic and genetically inherited PD. Interaction between aggregated αSyn (αSyn_{Agg}) and microglial immune receptors, such as the pattern recognition receptors TLR2 and CD36, on microglial plasma membranes can lead to microglial activation (7). Furthermore, αSyn has been demonstrated to induce IL-1β production in monocytes (8, 9) and microglia (10). However, much remains unknown regarding the key signaling pathways involved in either αSyn_{Agg}-mediated neuroinflammation in the nigral dopaminergic system (11, 12) or in chronic inflammation in microglia.

A voltage-gated potassium channel with the biophysical properties of Kv1.3 (13, 14) was first described in T cells (15, 16) but has since also been identified in B lymphocytes and macrophages, retinal ganglion cells, microglia, and neurons, where Kv1.3 is mostly part of heteromultimers with other Kv1 family members (17). Like the other 40 voltage-gated potassium channels found in humans, Kv1.3 consists of 4 α subunits, each with 6 transmembrane segments (S1–S6) and a voltage sensor in the S4 segment that is

Conflict of interest: AGK and VA have an equity interest in PK Biosciences Corporation located in Ames, Iowa, USA. The terms of this arrangement have been reviewed and approved by ISU in accordance with its conflict-of-interest policies. HW is an inventor on a 2004 University of California patent claiming PAP-1 as an immunosuppressant (5-Phenoxyalkoxypsoralens and methods for selective inhibition of the voltage-gated Kv1.3 potassium channel, patent no. US7557138B2).

Submitted: January 9, 2020; **Accepted:** April 29, 2020; **Published:** June 29, 2020.
Reference information: *J Clin Invest*. 2020;130(8):4195–4212.
https://doi.org/10.1172/JCI136174.

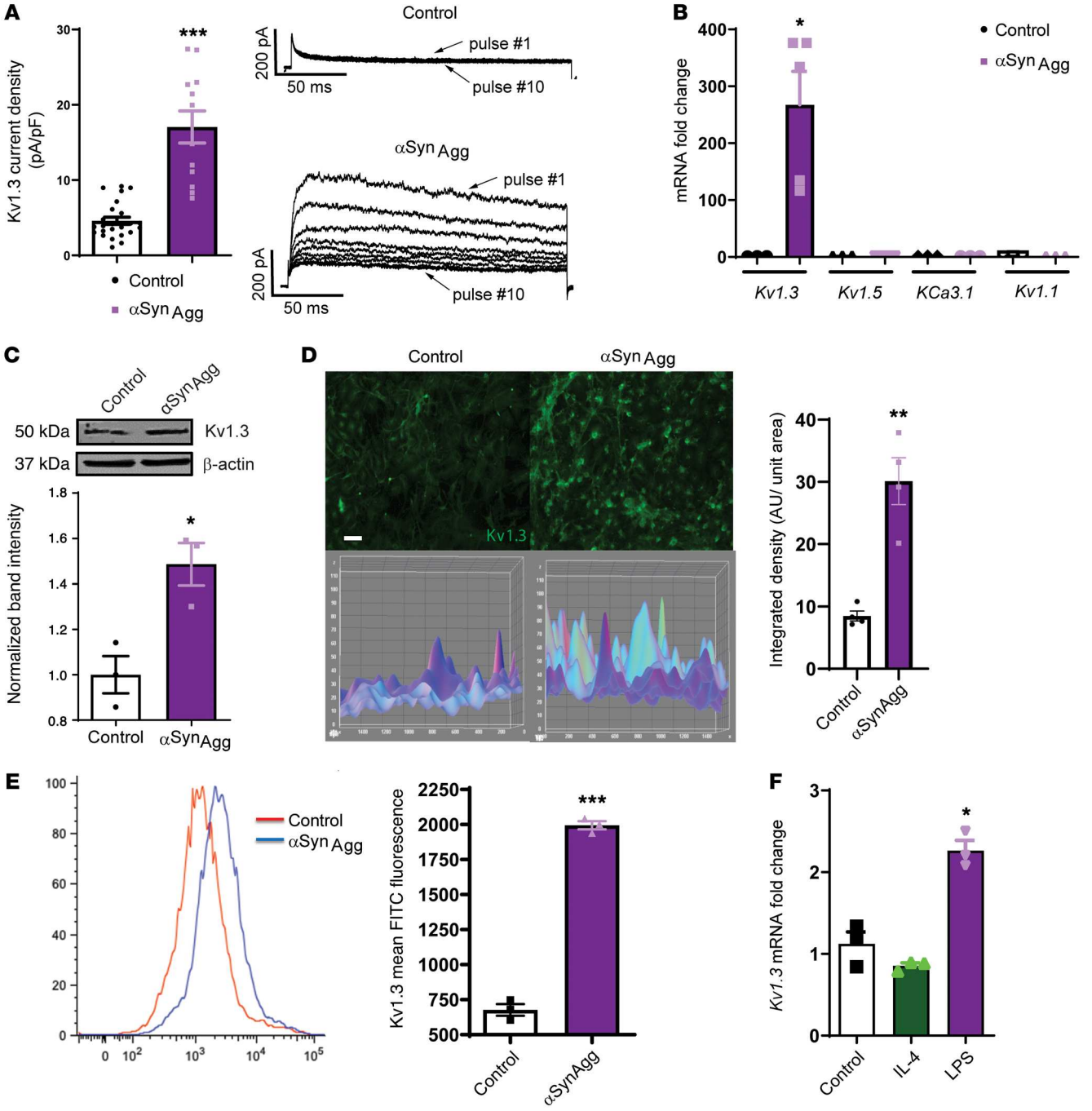

Figure 1. Upregulated expression of the potassium channel Kv1.3 upon aggregated αSyn stimulation in microglial cells in vitro. (**A**) Whole-cell patch-clamp recordings of PMCs treated with 1 μM αSyn_{Agg} for 24–48 hours, showing αSyn_{Agg}-induced increased Kv1.3 activity (control $n = 24$ and αSyn_{Agg} $n = 12$). Kv1.3 was identified by its characteristic use dependence, which was revealed when applying a train of ten 200-ms pulses from –80 to 40 mV at 1-second intervals (1 Hz). (**B**) qRT-PCR showing that αSyn_{Agg} induced *Kv1.3* mRNA expression without significantly altering other potassium channels. (**C**) Western blot of αSyn_{Agg}-induced Kv1.3 protein expression in PMCs. (**D**) ICC of αSyn_{Agg}-induced Kv1.3 protein expression in PMCs. Scale bar: 100 μm. (**E**) Flow cytometric analysis of immortalized MMCs treated with 1 μM αSyn_{Agg} for 24 hours, showing αSyn_{Agg}-induced Kv1.3 surface expression. (**F**) qRT-PCR of human microglia treated with LPS (1 μg/mL) and IL-4 (20 ng/mL) for 6 hours, showing LPS-induced Kv1.3 expression. A 1-way ANOVA was used to compare multiple groups. In most cases, Tukey's post hoc analysis was applied in **B** and **F**. A 2-tailed Student's *t* test was used for all other figures when comparing 2 groups. Each dot on the bar graphs represents a biological replicate. Data are presented as the mean ± SEM, with 3–5 biological replicates from 2–3 independent experiments unless otherwise noted. $^*P \le 0.05$, $^{**}P < 0.01$, and $^{***}P < 0.001$.

responsible for opening the channel in response to membrane depolarization. Kv1.3-KO mice are resistant to diet-induced obesity (18, 19) and experimental autoimmune encephalomyelitis (20) and also exhibit enhanced olfaction (21). These findings reveal the diverse functions of this voltage-gated channel, though its investigation has mostly been limited to autoimmune diseases. Kv1.3 also plays an important role in microglia-mediated neuronal cell death (22) and inflammatory cytokine production by microglia in

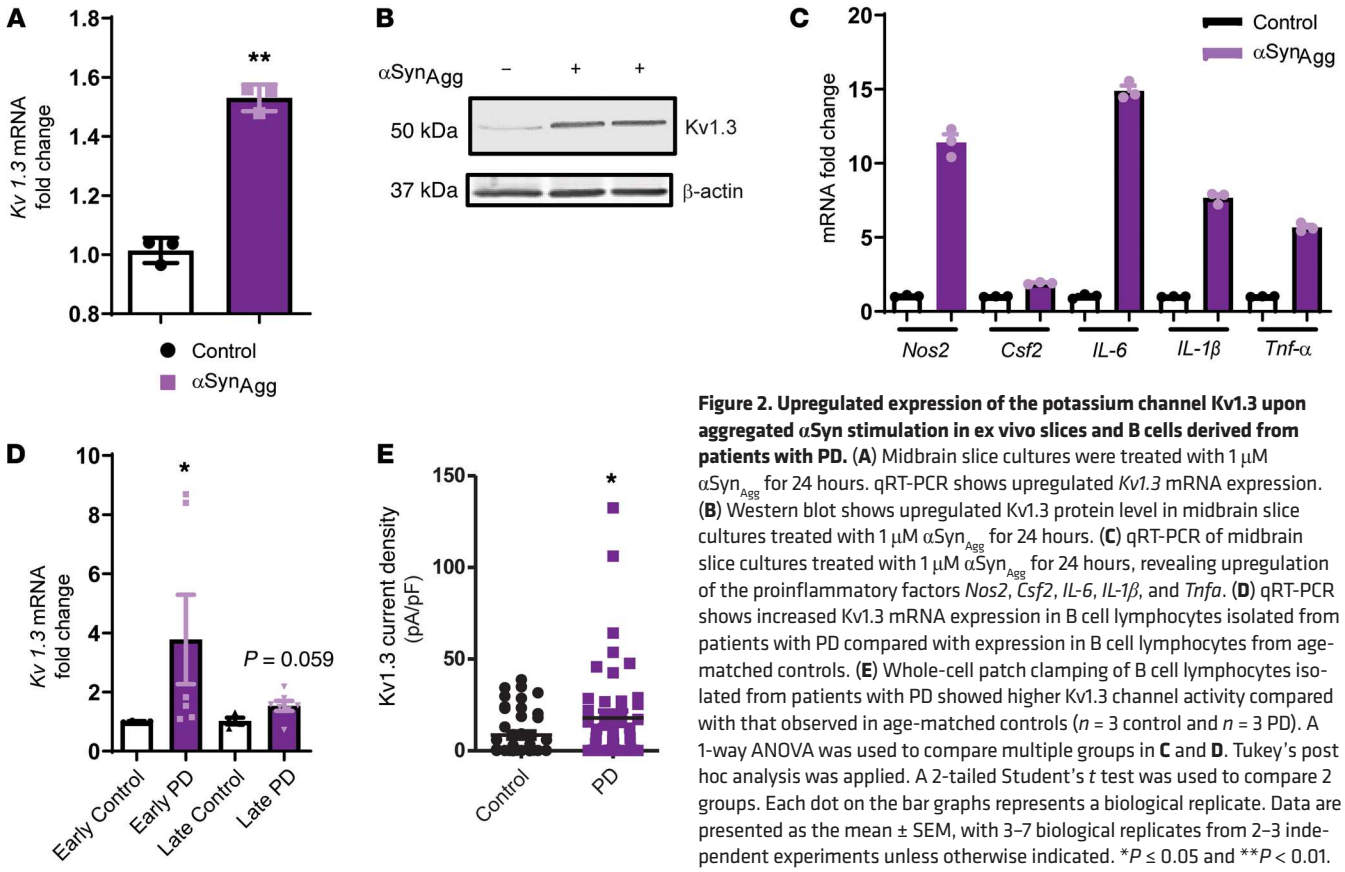

Figure 2. Upregulated expression of the potassium channel Kv1.3 upon aggregated αSyn stimulation in ex vivo slices and B cells derived from patients with PD. (**A**) Midbrain slice cultures were treated with 1 μM $αSyn_{Agg}$ for 24 hours. qRT-PCR shows upregulated *Kv1.3* mRNA expression. (**B**) Western blot shows upregulated Kv1.3 protein level in midbrain slice cultures treated with 1 μM $αSyn_{Agg}$ for 24 hours. (**C**) qRT-PCR of midbrain slice cultures treated with 1 μM $αSyn_{Agg}$ for 24 hours, revealing upregulation of the proinflammatory factors *Nos2*, *Csf2*, *IL-6*, *IL-1β*, and *Tnfa*. (**D**) qRT-PCR shows increased Kv1.3 mRNA expression in B cell lymphocytes isolated from patients with PD compared with expression in B cell lymphocytes from age-matched controls. (**E**) Whole-cell patch clamping of B cell lymphocytes isolated from patients with PD showed higher Kv1.3 channel activity compared with that observed in age-matched controls (n = 3 control and n = 3 PD). A 1-way ANOVA was used to compare multiple groups in **C** and **D**. Tukey's post hoc analysis was applied. A 2-tailed Student's t test was used to compare 2 groups. Each dot on the bar graphs represents a biological replicate. Data are presented as the mean ± SEM, with 3–7 biological replicates from 2–3 independent experiments unless otherwise indicated. *$P \leq 0.05$ and **$P < 0.01$.

vitro and in vivo (23, 24). Recently, Kv1.3 was shown to be upregulated in the postmortem brains of patients with Alzheimer's disease (AD) (25) and has been suggested to act as a pharmacological target for suppressing AD-associated neuroinflammation, based on work in AD mouse models (26). Interestingly, Kv1.3 contains multiple proline-rich sequences to which Src homology (SH) domains can bind, and recently, our laboratory showed that Fyn, a Src family kinase, is upregulated in PD models as well as in human PD nigral tissues and plays an important role in microglial inflammation (10, 27). Thus, we hypothesized that Fyn and Kv1.3 interact to augment the neuroinflammatory response, thereby regulating neurodegeneration in PD.

In this study, we investigated the role of microglial Kv1.3 in PD pathology and the transcriptional and posttranslational modifications of this channel in PD models. Our in vitro studies showed that Kv1.3 was highly upregulated in microglial cells treated with the PD-specific antigen $αSyn_{Agg}$. Kv1.3 was also upregulated in multiple animal models of PD and in postmortem human PD brains. Kv1.3 upregulation was not confined to the brain in humans, as lymphocytes isolated from patients with PD contained higher levels of Kv1.3 than did those obtained from control subjects, making it a potential biomarker. Furthermore, we report that Fyn could regulate Kv1.3 both transcriptionally and posttranslationally, thereby modulating its functional activity. Last, PAP-1, a small-molecule inhibitor of Kv1.3 that can cross the blood-brain barrier (26, 28), was able to reduce neuroinflammation and neurodegeneration in cell cultures and animal models of PD. We believe our findings have significant translational implications for the therapeutic treatment of PD.

Results

Upregulation of Kv1.3 potassium channel expression upon $αSyn_{Agg}$ stimulation in microglial cells and PD immune cells. Since Kv1.3 expression has been reported to increase in cultured microglia following stimulation with oligomeric amyloid-β and in the brains of AD mouse models and patients with AD (25, 26), we tested whether $αSyn_{Agg}$, which contributes to chronic neuroinflammation by activating microglia in PD (10, 27, 29), induces a similar increase in Kv1.3 expression. We therefore established mixed glial cultures from neonatal mice and treated primary microglia (PMCs) with 1 μM $αSyn_{Agg}$ for 24 to 48 hours. Whole-cell patch clamping revealed that $αSyn_{Agg}$ treatment increased functional Kv1.3 channel activity (Figure 1A). Parallel quantitative reverse transcription PCR (qRT-PCR) analysis showed that $αSyn_{Agg}$ most significantly induced *Kv1.3* mRNA expression compared with other potassium channels such as *KCa3.1*, *Kv1.1*, or *Kv1.5* (Figure 1B). Likewise, the Kv1.3 protein level also increased, as revealed by Western blot analysis (Figure 1C) and immunocytochemistry (ICC) (Figure 1D). Furthermore, flow cytometric analysis using a FITC-labeled Kv1.3 antibody against an extracellular epitope showed that $αSyn_{Agg}$ increased the surface expression of Kv1.3 (Figure 1E) in PMCs, in keeping with the observed increases in current density observed by electrophysiology (Figure 1A). Next, we corroborated each of our PMC findings using a line of mouse microglial cells (MMCs) for qRT-PCR (Supplemental Figure 1A; supplemental material available online with this article; https://doi.org/10.1172/JCI136174DS1), ICC (Supplemental Figure 1B), and Western blot (Supplemental Figure 1C) analyses. Moreover, whole-cell patch clamping confirmed that

treatment with the potent microglia activator LPS also upregulated Kv1.3 channel activity in PMCs (Supplemental Figure 1D), and flow cytometry revealed increased surface expression of Kv1.3 in MMCs (Supplemental Figure 1E), indicating that the observed upregulation of Kv1.3 may play a role in mediating microglial activation. After treating the MMCs with LPS (1 μg/mL) and IL-4 (20 ng/mL) for 6 hours to induce classical and alternative microglial activation, respectively, we observed that LPS induced *Kv1.3* mRNA expression, whereas IL-4 did not alter Kv1.3 expression (Figure 1F), further validating the finding that this voltage-gated potassium channel is related to the classical, proinflammatory activation of microglia (23). Following our in vitro studies of microglial cultures, we next adopted an ex vivo organotypic midbrain slice culture model, wherein a 24-hour exposure to 1 μM αSyn_{Agg} significantly induced the expression of *Kv1.3* mRNA (Figure 2A) and protein (Figure 2B) as well as mRNA expression of the proinflammatory genes *Nos2, Csf2, IL-6, IL-1β and Tnf-α* (Figure 2C). Next, we assessed mRNA expression of *Kv1.3* in PD patient– and control-derived B lymphocytic cells. Interestingly, we detected a significant increase in *Kv1.3* mRNA expression in PD patient–derived B lymphocytic cells compared with expression in age-matched control cells (Figure 2D). Importantly, the increase observed in the lymphocytic cells generated from patients with early-phase PD was much more robust than that detected in late-phase PD patient–derived cells, suggesting that lymphocytic Kv1.3 could be a potential biomarker for early PD diagnosis. Last, whole-cell patch clamping revealed that lymphocytes from patients with PD had higher Kv1.3 channel activity than did B lymphocytes from age-matched controls (Figure 2E). Collectively, these findings demonstrate that inflammatory stimuli, such as αSyn_{Agg} or LPS, induce functionally relevant increases in microglial Kv1.3 protein and mRNA levels, as indicated by the enhanced channel activity in microglial cells. Given the critical role of neuroinflammation in PD, these data suggest a possible role of Kv1.3 in PD pathogenesis and progression.

Kv1.3 channel expression is highly induced in microglial cells in experimental in vivo models of PD and in postmortem human PD brains. PD is a multifactorial disease, and to date no in vivo models can reproduce all the symptoms of PD. Hence, to better understand the potential role of Kv1.3, we used multiple animal models of PD to recapitulate various clinical and pathological aspects of the disease. One of the major pathological hallmarks of PD is protein aggregation, which can be recapitulated in the αSyn–adeno-associated virus (αSyn-AAV) mouse model (30), in which αSyn-AAV was stereotaxically injected into the striatum, and the mice were sacrificed 6 months later (Supplemental Figure 2A). Western blot analysis revealed a substantial induction of Kv1.3 in this animal model of PD (Figure 3A).

To verify whether Kv1.3 channel expression is induced in a more gradually progressive PD model, we used the MitoPark transgenic mouse model. MitoPark mice were developed by inactivating the mitochondrial transcription factor A (TFAM) in dopaminergic neurons (31) to model the mitochondrial dysfunction exhibited by the progressively neurodegenerative Parkinsonian syndrome, with its diverse spectrum of motor and nonmotor symptoms. We recently reported the activation of the NLRP3 inflammasome in this model, demonstrating the involvement of neuroinflammatory processes in nigral dopaminergic neuronal degeneration (32). Here, we show that *Kv1.3* gene expression was highly induced in the substantia nigra (SN) of 16- and 24-week old MitoPark mice compared with expression in age-matched littermate controls (Figure 3B). Our Western blot analysis further revealed that Kv1.3 was upregulated in the SN region in 24-week-old MitoPark mice (Figure 3C), and we confirmed that this upregulation was localized to IBA1-positive SN microglia (Figure 3D).

Next, we adopted the well-characterized subacute 1-methyl-4-phenyl-1,2,3,6-tetrahydropyridine (MPTP) model of Parkinsonism, in which mice received 20 mg/kg MPTP daily for 4 consecutive days and were sacrificed on the fifth day (Supplemental Figure 2B). In line with the αSyn-AAV and MitoPark models, we found that MPTP substantially increased mRNA and protein expression of nigral *Kv1.3* (Figure 3, E and F). Although MPTP treatment did not induce substantial αSyn aggregation in mouse models, a few reports have indicated that MPTP can induce αSyn upregulation and aggregation in nonhuman and rodent models (33, 34). It is likely that MPTP-induced mitochondrial dysfunction contributed to the upregulation of Kv1.3.

To further establish the clinical relevance of Kv1.3 in the Parkinsonian syndrome, we assessed Kv1.3 channel expression in postmortem human brains from patients with PD and patients with dementia with Lewy bodies (DLBs). When comparing striatal brain samples, we observed *Kv1.3* mRNA levels that were higher in postmortem human PD brains than in control brains (Figure 3G). Western blot analysis of tissues from PD and age-matched controls further showed increased Kv1.3 levels in the SN (Figure 3H). Immunostaining for Kv1.3 and IBA1 further showed upregulated Kv1.3 immunoreactivity in the prefrontal cortex (Figure 3I, top panels) and SN (Figure 3I, bottom panels) of PD brain sections that was localized to IBA1-positive microglia (Supplemental Figure 2C). We also examined Kv1.3 expression in another Parkinsonism-related synucleinopathy, DLB. Histochemical analysis of postmortem DLB brains (SN region) revealed that Kv1.3 expression had substantially increased in HLA-DR–positive microglial cells (Figure 3J) compared with expression in control brains. Together, these findings demonstrate that microglial Kv1.3 is highly induced in both animal models and patients with PD.

Fyn modulates the transcriptional regulation of Kv1.3 in microglial cells through the Fyn/PKCδ kinase signaling cascade. After confirming the expression of Kv1.3 in cell culture and various animal models of PD as well as in patients with PD, we investigated the molecular mechanism behind the transcriptional upregulation of the *Kv1.3* gene. Though a recent study demonstrated epigenetic regulation of Kv1.3 (35), its transcriptional regulation is not well understood. Our in silico analysis of the Kv1.3 promoter revealed multiple NF-κB and SP1 binding sites (Figure 4A), and previous studies showed that SP1 phosphorylation is dependent on the p38 MAPK pathway and that p38 MAPK is usually upstream of NF-κB (36, 37). We used the cell-permeable NF-κB inhibitor SN50 and the p38 MAPK inhibitor SB203580. Both inhibitors independently attenuated αSyn_{Agg}-induced *Kv1.3* upregulation in the microglial cell line (Figure 4B). These findings suggest that NF-κB and p38 MAPK signaling pathways contributed to the αSyn_{Agg}-induced Kv1.3 upregulation. We previously demonstrated that Fyn acts as an upstream regulator of the NF-κB transcription factor by regulating the nuclear translocation of p65 (27). Fyn has also been shown

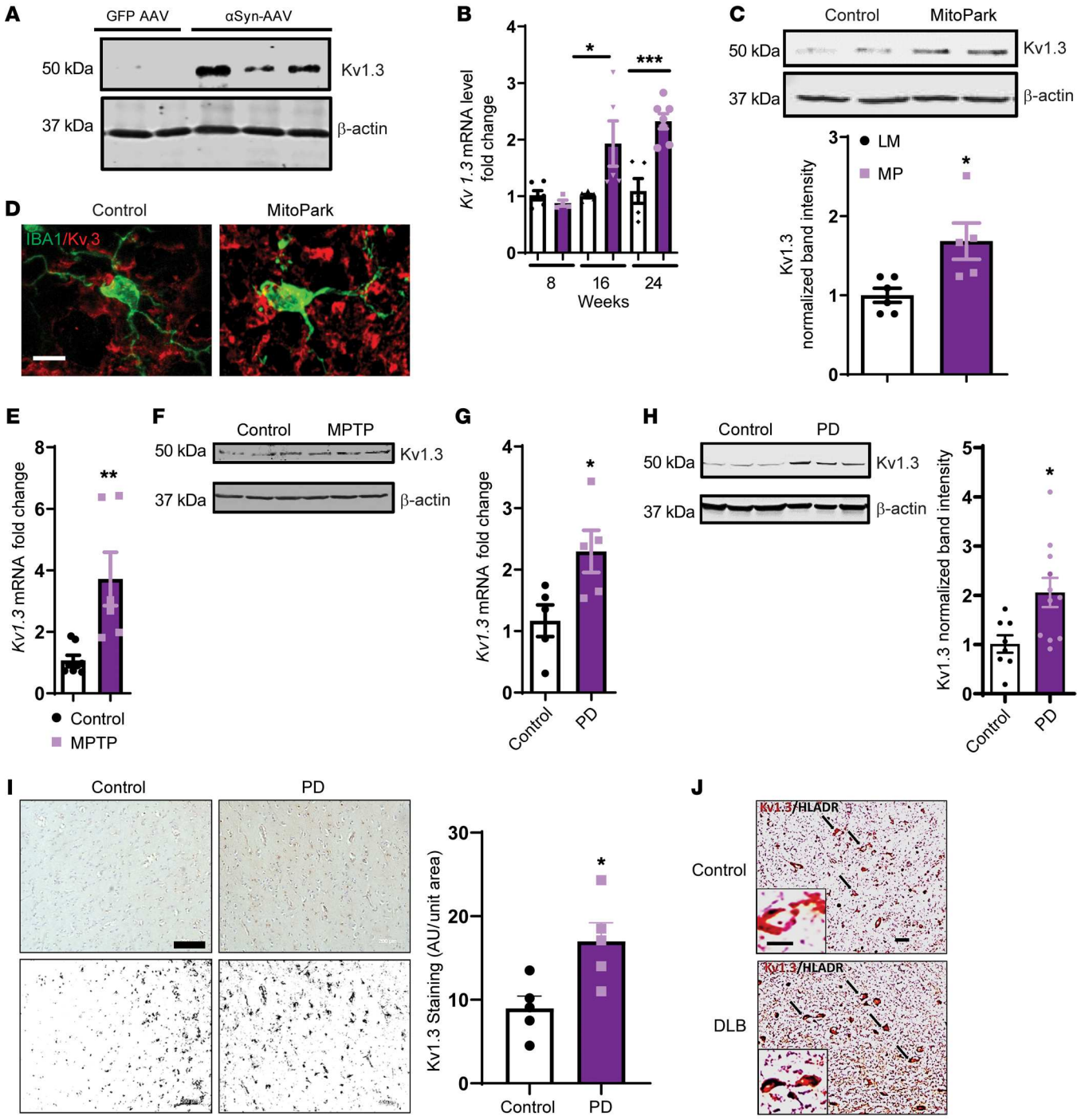

Figure 3. Kv1.3 expression is highly induced in microglial cells in experimental models of PD and postmortem PD brains. (**A**) Western blot showing increased Kv1.3 protein levels in the substantia nigra of the Syn-AAV mouse model of PD. (**B**) qRT-PCR analysis of 8- to 24-week-old nigral tissues from the MitoPark mouse model of PD showing Kv1.3 induction compared with age-matched littermate controls. (**C**) Western blot of 24-week-old nigral tissues from the MitoPark mouse model of PD (MP) showing induction of Kv1.3 protein expression compared with age-matched littermate control mice (LM). (**D**) IHC in 24-week-old nigral tissues from the MitoPark mouse model of PD showing higher Kv1.3 protein levels (red) in IBA1-positive microglial cells (green) compared with age-matched controls as revealed by their colocalization (yellow). Scale bar: 20 μm. (**E**) qRT-PCR analysis of nigral tissues from the MPTP mouse model revealing induction of Kv1.3 mRNA expression. (**F**) Western blot showing increased Kv1.3 protein levels in substantia nigra of the MPTP mouse model of PD. (**G**) qRT-PCR analysis of postmortem human PD brains showing elevated *Kv1.3* mRNA expression. (**H**) Western blot of the SN region of postmortem human PD brain showing induction of Kv1.3 protein expression compared with age-matched controls. $n = 6–8$. (**I**) Immunostaining revealing higher Kv1.3 levels in the prefrontal cortex of postmortem human PD brains compared with age-matched controls. Lower panel shows the deconvoluted binary image used for analysis. Three regions per brain were analyzed. Scale bar: 200 μm. (**J**) Dual DAB staining showing induction of Kv1.3 expression in HLA-DR–positive microglial cells in patients with DLBs compared with age-matched controls. Scale bars: 100 μm; 20 μm (enlarged insets). A 1-way ANOVA was used to compare multiple groups. Tukey's post hoc analysis was applied **B**. A 2-tailed Student's *t* test was used to compare 2 groups. Each dot on the bar graphs represents a biological replicate. Data are presented as the mean ± SEM, with 3–9 biological replicates from 2–3 independent experiments unless otherwise indicated. $^*P \le 0.05$, $^{**}P < 0.01$, and $^{***}P < 0.001$.

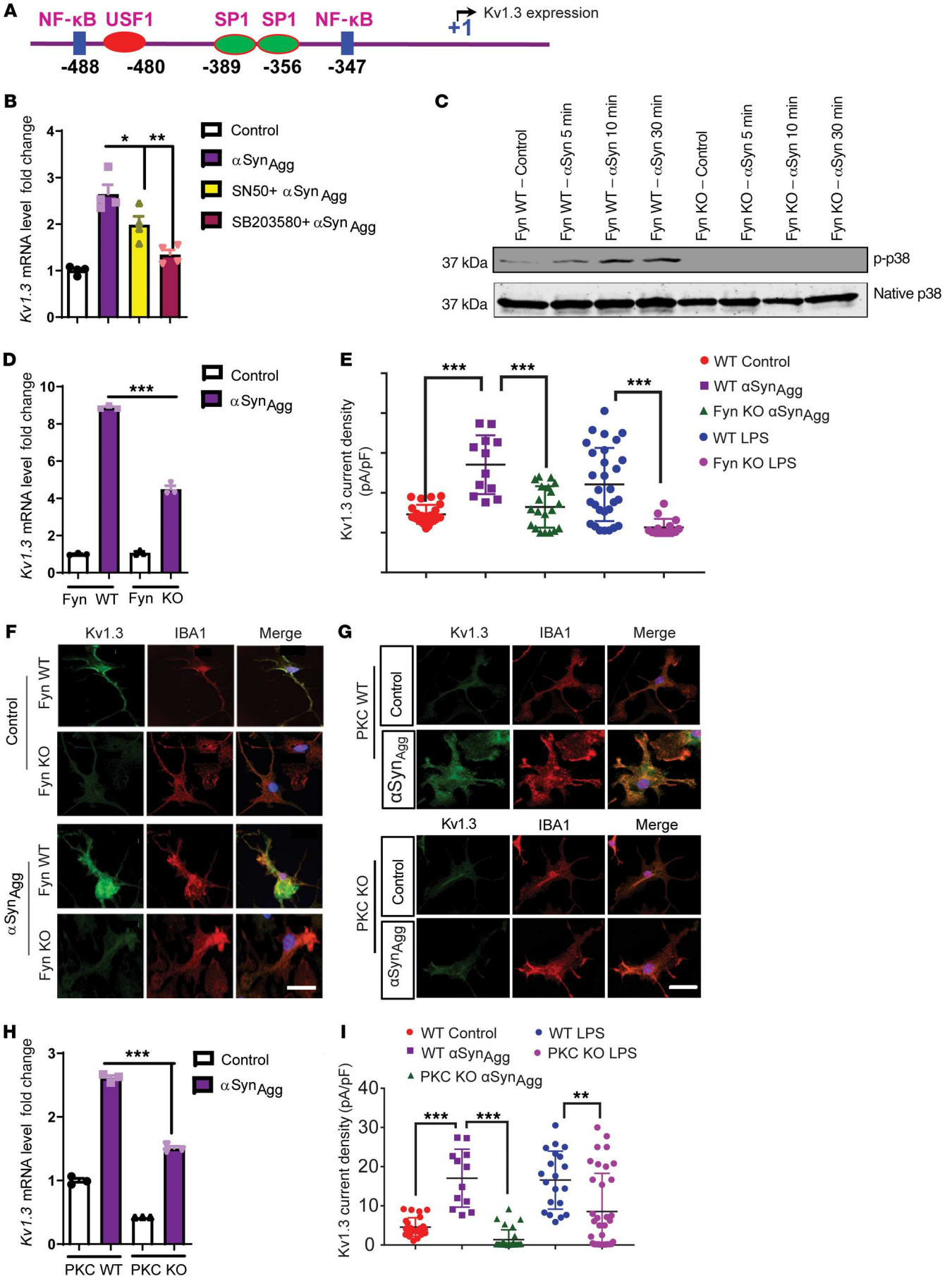
A
NF-κB USF1 SP1 SP1 NF-κB
Kv1.3 expression
+1
-488 -480 -389 -356 -347
B
Kv1.3 mRNA level fold change
Control
αSynAgg
SN50+ αSynAgg
SB203580+ αSynAgg
C
Fyn WT – Control
Fyn WT – αSyn 5 min
Fyn WT – αSyn 10 min
Fyn WT – αSyn 30 min
Fyn KO – Control
Fyn KO – αSyn 5 min
Fyn KO – αSyn 10 min
Fyn KO – αSyn 30 min
37 kDa
p-p38
37 kDa
Native p38
D
Kv1.3 mRNA level fold change
Control
αSynAgg
Fyn WT Fyn KO
E
Kv1.3 current density (pA/pF)
WT Control
WT αSynAgg
Fyn KO αSynAgg
WT LPS
Fyn KO LPS
F
Kv1.3 IBA1 Merge
Control
Fyn WT
Fyn KO
αSynAgg
Fyn WT
Fyn KO
G
Kv1.3 IBA1 Merge
PKC WT
Control
αSynAgg
PKC KO
Control
αSynAgg
H
Kv1.3 mRNA level fold change
Control
αSynAgg
PKC WT PKC KO
I
WT Control
WT αSynAgg
PKC KO αSynAgg
WT LPS
PKC KO LPS
Kv1.3 current density (pA/pF)

Figure 4. Fyn modulates the transcriptional regulation of Kv1.3 in microglial cells through the Fyn/PKCδ kinase signaling cascade. (**A**) In silico analysis of the promoter sequence of Kv1.3 revealed probable Nf-κB– and SP1-binding sites. (**B**) qRT-PCR analysis of immortalized MMCs cotreated with αSyn_{Agg} and either SN50 (100 μg/mL) or SB203580 (1 μM), showing that both compounds attenuated αSyn_{Agg}-induced Kv1.3 expression. (**C**) Western blot of Fyn WT and KO PMCs treated with αSyn_{Agg}, showing that Fyn KO reduced the induction of the p38 MAPK pathway. (**D**) qRT-PCR analysis revealed that Fyn KO reduced αSyn_{Agg}-induced *Kv1.3* mRNA levels. (**E**) Whole-cell patch-clamp recording showing that Fyn KO attenuated αSyn_{Agg}- and LPS-induced Kv1.3 activity compared with Fyn WT PMCs (WT control $n = 24$, WT αSyn_{Agg} $n = 12$, WT LPS $n = 29$, Fyn KO αSyn_{Agg} $n = 20$, Fyn KO LPS $n = 15$). (**F**) ICC showing that Fyn KO reduced αSyn_{Agg}-induced Kv1.3 protein levels in PMCs. Scale bar: 15 μm. (**G**) ICC of PMCs revealed that αSyn_{Agg}-induced Kv1.3 protein expression was reduced by PKCδ KO. Scale bar: 15 μm. (**H**) qRT-PCR analysis of PMCs showing that PKC KO reduced the expression of αSyn_{Agg}-induced *Kv1.3* mRNA. (**I**) Whole-cell patch clam recording of PMCs showing that PKC KO attenuated αSyn_{Agg}- and LPS-induced Kv1.3 activity compared with PKC WT PMCs (WT control $n = 24$, WT αSyn_{Agg} $n = 12$, WT LPS $n = 20$, PKC-KO αSyn_{Agg} $n = 29$, PKC-KO LPS $n = 35$). Data are presented as the mean ± SD. A 1-way ANOVA was used to compare multiple groups. In most cases, Tukey's post hoc analysis was applied. Each dot on the bar graphs represents a biological replicate. Data are presented as the mean ± SEM, with 3–4 biological replicates from 2–3 independent experiments unless otherwise indicated. $^{*}P \leq 0.05$, $^{**}P < 0.01$, and $^{***}P < 0.001$.

to modulate LPS-induced activation of the p38 MAPK pathway. Indeed, our Western blot analysis of PMC cultures revealed that knocking out Fyn in PMCs attenuated αSyn_{Agg}-induced p38 phosphorylation (Figure 4C), further demonstrating that Fyn acts upstream of p38 MAPK activation following αSyn_{Agg} stimulation. Accordingly, we hypothesized that Fyn may regulate inflammagen-induced Kv1.3 upregulation. Fyn deficiency in PMCs attenuated αSyn_{Agg}-induced *Kv1.3* expression, as revealed by qRT-PCR (Figure 4D) and ICC (Figure 4F) analyses. Importantly, a whole-cell patch-clamp study of LPS- and αSyn_{Agg}-treated microglial cells revealed that Fyn-KO microglia had lower Kv1.3 current density than did WT microglia (Figure 4E). Next, we pharmacologically inhibited Fyn in αSyn_{Agg}-stimulated PMCs by cotreating them with the potent Src family kinase inhibitor saracatinib (1 μM). Electrophysiological analysis revealed that saracatinib treatment reduced both LPS- and αSyn_{Agg}-induced Kv1.3 channel activity, further suggesting the probable role of Fyn in modulating Kv1.3 activity (Supplemental Figure 3A). As revealed by qRT-PCR analyses, cotreatment with saracatinib reduced αSyn_{Agg}-induced expression of *Kv1.3* (Supplemental Figure 3B) as well as expression of the proinflammatory gene *Nos2* (Supplemental Figure 3C) and the cytokines TNF-α and IL-1β (Supplemental Figure 3, E and F), without altering mRNA expression of *Fyn* itself (Supplemental Figure 3D).

Our group recently showed that PKCδ, a serine/threonine kinase involved in microglial inflammation (38), is modulated by Fyn (27). We have previously shown that Fyn can directly modulate PKCδ, which can induce the activation of p38 MAPK and the nuclear translocation of p65 (27). To further show whether Kv1.3 expression is dependent on the Fyn/PKCδ signaling axis, we treated PMCs with 1 μM αSyn_{Agg} for 1 hour, followed by ICC (Figure 4G) and qRT-PCR (Figure 4H), which revealed that PKCδ deficiency attenuated αSyn_{Agg}-induced Kv1.3 mRNA and protein expression. Moreover, whole-cell patch clamping revealed that PKCδ deficiency reduced Kv1.3 current density in microglia treated with either αSyn_{Agg} (1 μM) for 24 hours or LPS (300 ng/mL) for 48 hours (Figure 4I). These findings collectively suggest that the Fyn/PKCδ kinase signaling cascade plays a crucial role in Kv1.3 upregulation in response to inflammatory stimuli.

Fyn modulates posttranslational modification of Kv1.3. Posttranslational modification of Kv1.3 activity and other cellular functions has been attributed to phosphorylation of serine/threonine residues or tyrosine residues by various kinases and dephosphorylation by phosphatases (39–42). Kv1.3 has proline-rich regions in its N-terminal and C-terminal ends, which can bind to the Src homology domain 3 (SH3) of Src kinases. We have linked Fyn to the regulation of microglial inflammation (27), which prompted us to hypothesize that Fyn plays an important role in regulating the phosphorylation profile of Kv1.3 (43). Our multiple sequence alignment using T-Coffee software (44) to align N-terminal Kv1.3 sequences from 7 different organisms demonstrated that Kv1.3 is highly conserved and that the tyrosine residue at 135 (187 in humans) is conserved in all species (Supplemental Figure 4). Interestingly, Western blot analyses of postmortem human brains revealed that patients with PD expressed significantly more pY135 Kv1.3 than age-matched controls (Figure 5A).

To verify whether Fyn directly interacts with Kv1.3, we performed co-IP assays. After treating PMCs with αSyn_{Agg} for 24 hours, Fyn and Kv1.3 were pulled down and probed for Kv1.3 and Fyn, respectively. Our immunoblot analysis revealed that Fyn interacted with Kv1.3 in αSyn_{Agg}-exposed PMCs (Figure 5B). We performed a proximity ligation assay (PLA) using Duolink, which further verified the interaction of Fyn with Kv1.3 (Figure 5C). We also treated PMCs from $Fyn^{+/+}$ and $Fyn^{-/-}$ mice with αSyn_{Agg}, and both Western blot (Figure 5D) and ICC (Supplemental Figure 5A) analyses revealed that the αSyn_{Agg}-induced upregulation of phosphorylated Kv1.3 (p-Kv1.3) at residue 135 was diminished in $Fyn^{-/-}$ microglia. This finding is in line with the whole-cell patch-clamp data in Figure 4E showing that αSyn_{Agg}- and LPS-treated $Fyn^{-/-}$ PMCs had reduced current compared with $Fyn^{+/+}$ cells. To add in vivo relevance, we performed IHC analysis on the previously described αSyn preformed fibrils (αSyn_{PFF}) model. Interestingly, injections of αSyn_{Agg} induced phosphorylation of Kv1.3 at Tyr35 in $Fyn^{+/+}$ mice, but this induction of phosphorylation was not evident in $Fyn^{-/-}$ mice, further demonstrating the role of Fyn in modulating the phosphorylation of Kv1.3 at Tyr135 (Figure 5E). Furthermore, we orally administered the Fyn inhibitor saracatinib to MitoPark mice aged 8–16 weeks every other day and then examined the phosphorylation status of Kv1.3. IHC analysis revealed that Fyn inhibition decreased p-Kv1.3 (Tyr135) in the SN region of 16-week-old MitoPark mice (Figure 5F). These data collectively suggest that Fyn directly phosphorylates Kv1.3 at residue 135 in PD models.

To further evaluate the role of this phosphorylation at residue 135 in αSyn_{Agg}-stimulated inflammatory responses, MMCs were transiently transfected with a Kv1.3 WT plasmid or a mutant plasmid, whereby the tyrosine residue at 135 was mutated to alanine. Following transfection, the cells were treated with 1 μM αSyn_{Agg} for 24 hours. Western blot analysis revealed that ectopic expression of the Kv1.3 mutant attenuated αSyn_{Agg}-induced upregulation of Kv1.3 phosphorylation (Supplemental Figure 5B), whereas the qRT-PCR, Griess, and Luminex anal-

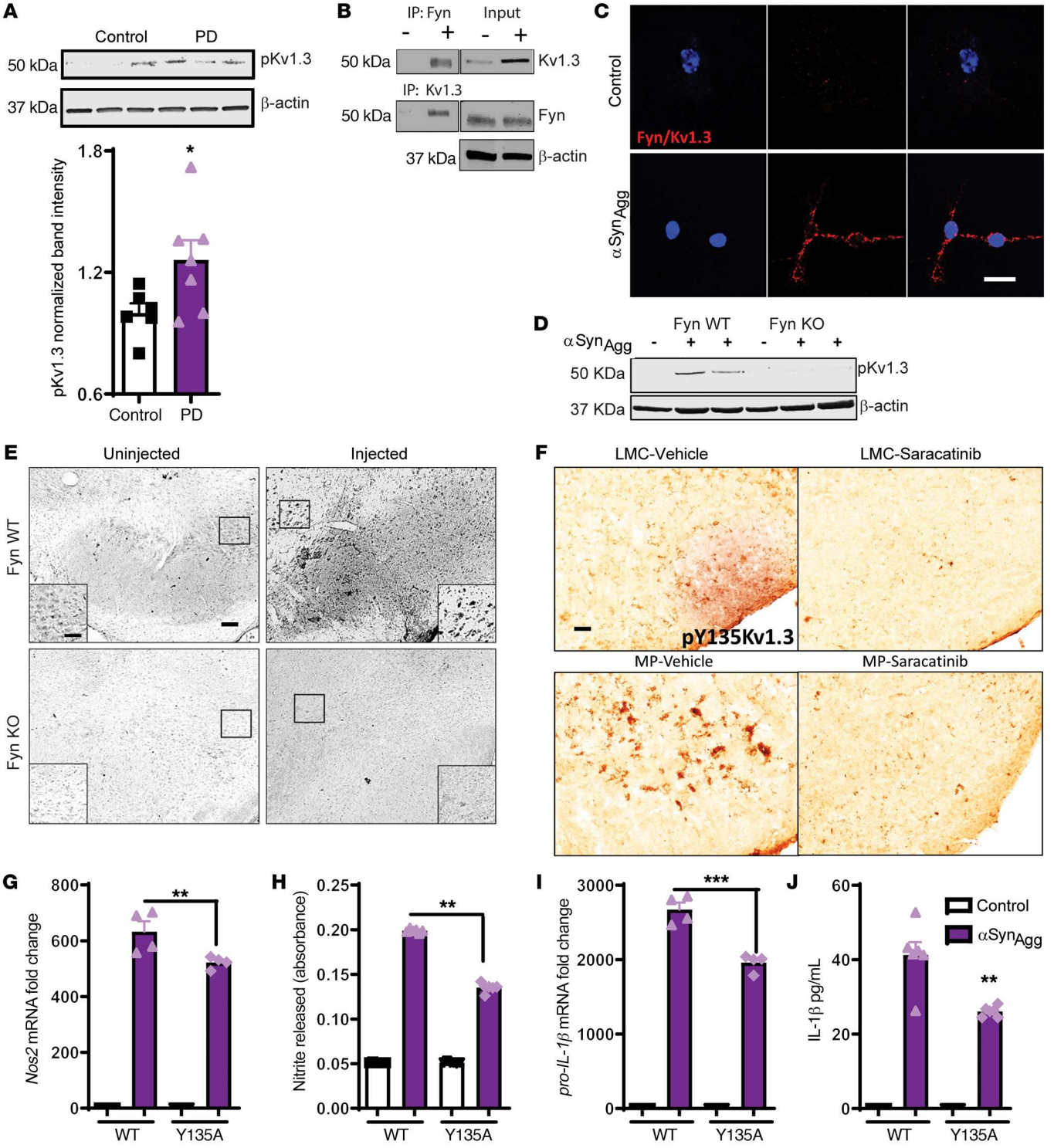

Figure 5. Fyn modulates the posttranslational modification of Kv1.3. (**A**) Western blot analysis of postmortem human PD and age-matched control brains showing increased phosphorylation of Kv1.3. (**B**) Immunoprecipitation of Fyn and Kv1.3 showing direct Fyn-Kv1.3 interaction after αSyn_{Agg} treatment. (**C**) Duolink PLA showing αSyn_{Agg}-induced interaction between Kv1.3 and Fyn. Scale bar: 25 μm. (**D**) Western blot of Fyn WT and KO PMCs revealed that Kv1.3 phosphorylation at residue 135 was Fyn dependent. (**E**) IHC analysis of substantia nigra from *Fyn*$^{+/+}$ and *Fyn*$^{-/-}$ mice showing reduced phosphorylation of Kv1.3 after αSyn_{PFF} injection. Scale bars: 100 μm; 60 μm (insets). (**F**) IHC of substantia nigra from MitoPark mice and their littermate controls showing that pharmacological inhibition of Fyn by saracatinib reduced Kv1.3 phosphorylation. Scale bar: 100 μm. (**G**–**J**) Immortalized MMCs were either transfected with WT Kv1.3 or aY135A Kv1.3 plasmid. (**G**) qRT-PCR analysis and (**H**) Griess assay showing reduced levels of inducible NOS (iNOS) and nitrite release, respectively, in Y135A Kv1.3-transfected cells compared with WT cells. (**I**) qRT-PCR analysis showing reduced IL-1β production in Y135A Kv1.3–transfected versus WT Kv1.3–transfected MMCs. (**J**) Luminex assay showing reduced IL-1β secretion in Y135A Kv1.3–transfected compared with WT Kv1.3–transfected MMCs. A 1-way ANOVA was used to compare multiple groups. In most cases, Tukey's post hoc analysis was applied. A 2-tailed Student's *t* test was used to compare 2 groups in **A**. Each dot on the bar graphs represents a biological replicate. Data are presented as the mean ± SEM, with 3–4 biological replicates from 2–3 independent experiments. $^*P \le 0.05$, $^{**}P < 0.01$, and $^{***}P < 0.001$.

yses further revealed reduced αSyn_{Agg}-induced upregulation of *Nos2* mRNA (Figure 5G), nitrite release (Figure 5H), and the proinflammatory cytokine IL-1β (Figure 5, I and J). Together, these results suggest that Fyn phosphorylates Kv1.3 at residue 135 and that this Fyn-induced phosphorylation plays a role in Kv1.3-mediated inflammation in PD models.

Kv1.3 modulates neuroinflammation in a cell culture model of PD. To demonstrate the role of Kv1.3 in αSyn_{Agg}-induced microglial activation, we performed a series of Kv1.3-KO and overexpression studies. PMCs from Kv1.3 WT and -KO animals were cultured and treated with αSyn_{Agg} for 24 hours. Luminex assays revealed that PMCs from Kv1.3-KO mice secreted significantly less TNF-α (Figure 6A), IL-12 (Figure 6B), and IL-1β (Figure 6C) than did WT PMCs. Next, we overexpressed Kv1.3 in MMCs (45) and treated them with αSyn_{Agg} for 24 hours. Our qRT-PCR analysis revealed that Kv1.3 overexpression (Supplemental Figure 6) significantly increased αSyn_{Agg}-induced mRNA levels of *Nos2* (Figure 6D), pro–*IL-1β* (Figure 6E), and *Tnf-α* (Figure 6F). Multiplex assays further revealed that Kv1.3 overexpression significantly induced the secretion of IL-6 (Figure 6G) and IL-12 (Figure 6H) following αSyn_{Agg} treatment. These data collectively suggest that $K_v1.3$ plays an important role in αSyn_{Agg}-induced microglial inflammation.

The small-molecule PAP-1 is a pharmacological inhibitor that specifically blocks Kv1.3 activity (28) and is known to reduce inflammation in rodent models of autoimmune disease. We cotreated PMCs with αSyn_{Agg} and PAP-1. Patch clamping showed that PAP-1 blocked Kv1.3 currents in αSyn_{Agg}-stimulated microglia (Figure 6I). A lactate dehydrogenase (LDH) assay revealed that PAP-1 blocked the αSyn_{Agg}-induced release of LDH into the extracellular space (Figure 6J). PAP-1 also significantly reduced the αSyn_{Agg}-induced release of the proinflammatory cytokines IL-12 (Figure 6K), TNF-α (Figure 6L), and IL-6 (Figure 6M) as revealed by Luminex multiplex cytokine analysis. To further demonstrate the efficacy of PAP-1 in reducing microglial inflammation, MMCs were cotreated with PAP-1 (1 μM) and αSyn_{Agg}. The Griess assay showed that PAP-1 reduced αSyn_{Agg}-induced nitrite release in these immortalized microglial cells (Supplemental Figure 7A), whereas qRT-PCR analysis showed that PAP-1 reduced expression of the αSyn_{Agg}-induced inflammatory genes *Nos2* (Supplemental Figure 7B), *IL-6* (Supplemental Figure 7C), *TNF-α* (Supplemental Figure 7D), and *IL-1β* (Supplemental Figure 7E). However, PAP-1 treatment did not induce the markers for alternative activation of microglia, *IRF4* (Supplemental Figure 7F) and *MRC1* (Supplemental Figure 7G). Luminex assays further demonstrated that PAP-1 could significantly attenuate αSyn_{Agg}-induced release of the proinflammatory cytokines IL-1β (Supplemental Figure 7H), TNF-α (Supplemental Figure 7I), and IL-6 (Supplemental Figure 7J).

To advance our understanding of the role of the Kv1.3-dependent signaling cascade in modulating neuroinflammation in microglia, we performed immunoblot analysis on PAP-1–treated MMCs. Western blot and ICC analyses demonstrated that PAP-1 significantly reduced αSyn_{Agg}-induced NLRP3 inflammasome protein upregulation (Figure 6, N and O). Together, these findings suggest that Kv1.3 contributes to classical microglial activation, which can be attenuated by PAP-1.

PAP-1 reduces neuroinflammation and neurodegeneration in mouse models of PD. PAP-1 and other Kv1.3 inhibitors have been widely used in animal models of inflammation including psoriasis (46), autoimmune diabetes (47), ischemic stroke (48), and AD (26), and its chronic administration is well tolerated in mice, rats, and primates (49). To validate the therapeutic potential of PAP-1 in Parkinsonian syndromes, we used the transgenic MitoPark progressive dopaminergic neurodegenerative model of PD and the toxin-based MPTP mouse model of PD.

MitoPark mice were injected daily with 40 mg/kg (i.p.) PAP-1 from ages 14 to 20 weeks (Supplemental Figure 8A). During treatment, no significant weight loss was observed (Supplemental Figure 8B). To verify the bioavailability and brain penetrance of PAP-1, we performed liquid chromatography–mass spectrometry (LC-MS) analysis of serum and brain samples taken at the end of the study and found that total PAP-1 serum and brain concentrations in the treated animals averaged 322 ± 122 nM and 848 ± 295 nM, respectively, 24 hours after the last administration (Supplemental Figure 8C). We detected no PAP-1 in the serum or brains of the vehicle-treated animals. Behavioral tests revealed that PAP-1 significantly reduced motor deficits in MitoPark mice (Figure 7, A–C). As evident from representative movement tracks (Figure 7A), PAP-1 treatment significantly increased horizontal activity in the open-field test (Figure 7B). PAP-1 also significantly increased the time spent on the rotarod by MitoPark mice (Figure 7C). Biochemical analysis of the striatum revealed that PAP-1 reduced loss of the neurotransmitter dopamine (Figure 7D) and its derivatives DOPAC (Figure 7E) and homovanillic acid (HVA) (Figure 7F) in MitoPark mice. Furthermore, stereological analysis demonstrated that PAP-1 significantly protected MitoPark mice from the loss of dopaminergic neurons (Figure 7G). Fluoro-Jade and IHC staining further revealed that PAP-1 reduced the extent of microgliosis and neuronal degeneration in MitoPark mice (Supplemental Figure 8D).

Next, we evaluated the efficacy of PAP-1 in protecting against MPTP-induced neuronal loss and inflammation (Supplemental Figure 9A). As expected, the LC-MS analysis revealed that PAP-1 crossed the blood-brain barrier (Supplemental Figure 9B). IHC analysis demonstrated that PAP-1 reduced MPTP-induced microgliosis in both the striatum and SN (Figure 7H). Skeletonization analysis (50) revealed that PAP-1 reduced microglial soma size and increased the number of branches compared with MPTP treatment alone (Figure 7I). Increased microglial soma size and decreased branch numbers are indicative of classical activation of microglia. Moreover, qRT-PCR analysis revealed that Kv1.3 inhibition reduced MPTP-induced expression of the proinflammatory cytokines TNF-α and pro–IL-1β (Figure 7J). Biochemical analysis showed that PAP-1 significantly increased the amount of dopamine (Supplemental Figure 9C) and its metabolites DOPAC (Supplemental Figure 9D) and HVA (Supplemental Figure 9E) compared with MPTP treatment alone. TH neuronal staining and stereological analysis further demonstrated that PAP-1 protected against MPTP-induced dopaminergic neuronal loss in the SN (Figure 7, K and L).

Finally, we also used the αSyn_{PFF} mouse model to further demonstrate the effect of Kv1.3 inhibition as a potential therapeutic target for PD. We injected αSyn_{PFF} into the striatum, and 4 months after injection, PAP-1 (40 mg/kg) was administered for 30 days (Figure 8A). As evident from representative movement tracks (Figure 8B), PAP-1 significantly decreased the rest time (Figure 8C) and increased horizontal activity (Figure 8D) and total distance

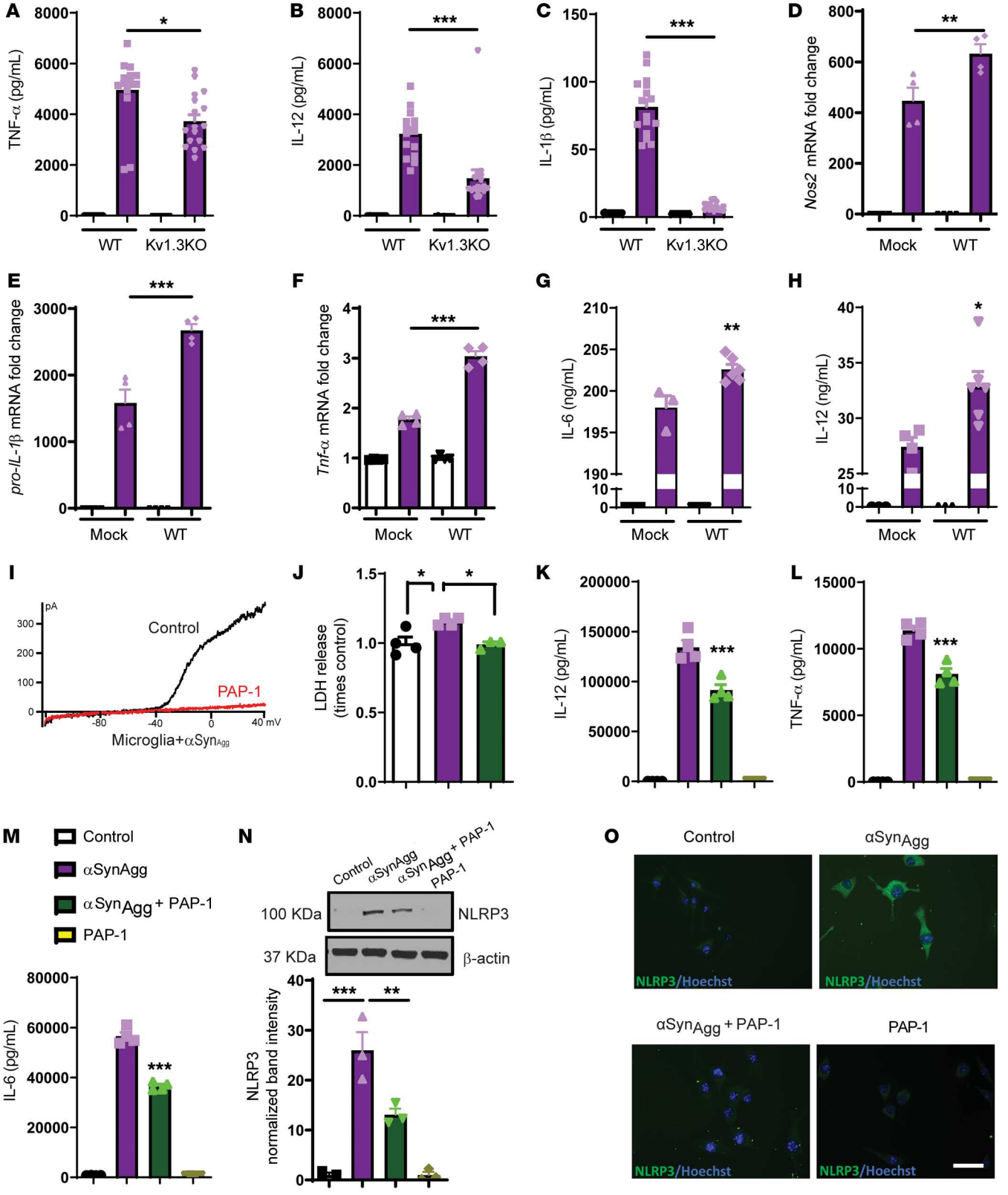
A
TNF-α (pg/mL)
WT
Kv1.3KO
B
IL-12 (pg/mL)
C
IL-1β (pg/mL)
D
Nos2 mRNA fold change
Mock
WT
E
pro-IL-1β mRNA fold change
F
Tnf-α mRNA fold change
G
IL-6 (ng/mL)
H
IL-12 (ng/mL)
I
pA
Control
PAP-1
Microglia+αSynAgg
J
LDH release (times control)
K
IL-12 (pg/mL)
L
TNF-α (pg/mL)
M
Control
αSynAgg
αSynAgg + PAP-1
PAP-1
IL-6 (pg/mL)
N
Control
αSynAgg
αSynAgg + PAP-1
PAP-1
100 KDa
NLRP3
37 KDa
β-actin
NLRP3 normalized band intensity
O
Control
αSynAgg
αSynAgg + PAP-1
PAP-1
NLRP3/Hoechst

Figure 6. Kv1.3 modulates neuroinflammation in a cell culture model of PD. (**A**–**C**) Kv1.3 WT and KO PMCs were treated with 1 μM αSyn_{Agg} for 24 hours. Luminex analysis shows that Kv1.3 KO reduced the release of the αSyn_{Agg}-induced proinflammatory factors (**A**) TNF-α, (**B**) IL-12, and (**C**) IL-1β. (**D**–**H**) Immortalized MMCs were transfected with WT a Kv1.3 plasmid, and then 48 hours after transfection, cells were treated with 1 μM αSyn_{Agg} for 24 hours. (**D**–**F**) qRT-PCR analysis showing that Kv1.3 overexpression aggravated αSyn_{Agg}-induced production of the proinflammatory factors (**D**) *Nos2*, (**E**) pro–*IL-1β*, and (**F**) *TNF-α*. (**G** and **H**) Luminex analysis showing that Kv1.3 overexpression potentiated the release of the proinflammatory factors (**G**) IL-6 and (**H**) IL-12. (**I**) Voltage ramp from –120 mV to 40 mV elicited a characteristic outward rectifying current in αSyn_{Agg}-treated microglia that was sensitive to the Kv1.3-selective inhibitor PAP-1. (**J**) LDH assay showing that PAP-1 reduced αSyn_{Agg}-induced LDH release from microglial cells. (**K**–**M**) Luminex assay revealing that PAP-1 attenuated the αSyn_{Agg}-induced proinflammatory factors (**K**) IL-12, (**L**) TNF-α, and (**M**) IL-6. (**N**) Western blot analysis demonstrating that PAP-1 reduced αSyn_{Agg}-induced NLRP3 expression. (**O**) ICC analysis revealed that PAP-1 reduced NLRP3 expression induced by αSyn_{Agg}. Scale bar: 25 μm. A 1-way ANOVA was performed to compare multiple groups. In most cases, Tukey's post hoc analysis was applied. Each dot on the bar graphs represents a biological replicate. Data are presented as the mean ± SEM, with 3–4 biological replicates from 2–3 independent experiments. $^*P \le 0.05$, $^{**}P < 0.01$, and $^{***}P < 0.001$.

traveled (Figure 8E). Furthermore, biochemical analysis revealed that PAP-1 restored the αSyn_{PFF}-induced loss of dopamine (Figure 8F) and its metabolite DOPAC (Figure 8G). Western blot analysis further confirmed that PAP-1 reduced the αSyn_{PFF}-induced loss of TH expression in the SNpc region of the brain (Figure 8H). Collectively, these preclinical studies suggest that PAP-1 can reduce microgliosis, inflammation, and neuronal loss in PD models and that inhibition of Kv1.3 by a brain-penetrant small molecule has clinical potential for PD treatment.

Discussion

Although neuroinflammation is one of the key pathophysiological hallmarks of neurodegenerative disorders, including PD, the molecular mechanisms and the key regulators of this chronic, sustained inflammation are not well understood (4). Recently, various antiinflammatory drugs targeting cellular pathways modulating inflammation have gained importance in clinical and preclinical trials in AD and PD (51, 52). In the present study, we demonstrate for the first time to our knowledge that the voltage-gated potassium channel Kv1.3 is upregulated in microglia in Parkinsonism. We showed previously that exposure to an inflammagen activates the Src family kinase Fyn, which regulates the p38 MAPK and the NF-κB pathways in microglial cells (27) and that Fyn phosphorylates PKCδ, a novel PKC isoform that also regulates the microglial NF-κB pathway (38). In this study, we reveal that both the p38 MAPK and the classical NF-κB pathways mediate the transcriptional regulation of Kv1.3. Furthermore, we identify the Fyn/PKCδ inflammatory pathway as a major regulator of Kv1.3 transcription in response to inflammatory stimuli. We demonstrate that the phosphorylation profile of Kv1.3 can be modulated by αSyn_{Agg} and that Fyn kinase plays an important role in this αSyn_{Agg}-induced Kv1.3 phosphorylation. Finally, we show that PAP-1, a brain-penetrant, small-molecule Kv1.3 inhibitor, can reduce neuroinflammation and neurodegeneration in multiple animal models of PD, demonstrating the translational relevance of our study.

The role of the microglial neuroinflammatory response in the neurodegenerative process of PD was first identified over 3 decades ago (53), but the exact molecular mechanism underlying the sustained inflammation remains unresolved. Meta-analyses have revealed that NSAIDs can protect against neurodegenerative disorders (54), suggesting that an effective translational strategy to dampen neuroinflammation could offer neuroprotection in PD. Recent studies have shown that αSyn_{Agg}, a major component of Lewy bodies and neurites, can be transferred from cell to cell in a prion-like manner, leading to the spread of disease pathology (55, 56). Although αSyn_{Agg} can induce inflammation in cell cultures and animal models of PD, the downstream signaling mechanism is not well understood (38). In this study, we show that the microglial Kv1.3 potassium channel was highly upregulated in response to αSyn_{Agg}. Interestingly, we show that surface Kv1.3 expression levels (Figure 1E) increased to a much greater degree than whole-cell protein levels (Figure 1C), suggesting that the trafficking of Kv1.3 to the surface plays an important role in this upregulation. Previous studies have reported that adaptor protein 1 (AP-1), which is responsible for clathrin-coated vesicle formation, governs Kv1.3 trafficking and that Fyn plays an important role in governing AP-1 expression (57, 58). Therefore, future studies looking into the role of the Fyn/AP-1 axis in αSyn_{Agg}-induced Kv1.3 trafficking are warranted. Currently, the exact reason for the difference in magnitude between Kv1.3 mRNA and protein upregulation is not entirely clear (Figure 1, B versus C), but it probably results from changes in Kv1.3 mRNA turnover, translational control, or the protein turnover rate. The difference could also be due to the higher sensitivity of a qRT-PCR–based mRNA assay compared with the semiquantitative Western blot method. We observed the induction of Kv1.3 in multiple in vivo models of PD, recapitulating various key hallmarks of PD. Moreover, we found that Kv1.3 was also upregulated in patients with Parkinsonian syndrome (PD and DLB), demonstrating the clinical relevance of our findings.

Ion channels play an important role in the immune system by regulating membrane potential and calcium signaling. The potassium channel Kv1.3, in particular, is widely regarded as a promising target for immunosuppression (59) and has been demonstrated to constitute a valid target for treating T cell–mediated autoimmune diseases in animal models of multiple sclerosis, autoimmune diabetes, rheumatoid arthritis, and psoriasis (47, 59). Kv1.3 blockers have also been shown to rescue neurogenesis by inhibiting granzyme B–releasing $CD8^+$ T cells (60). In microglial cells, the resident immune cells of the brain, Fordyce et al. (22) demonstrated that Kv1.3 is involved in microglia-mediated neuronal killing, whereas others (61) have implicated Kv1.3 in HIV-induced microglial neurotoxicity. More recently, 2 studies have shown that increased Kv1.3 expression in microglia is associated with classical "M1-like" activation (23) and that Kv1.3 is involved in modulating microglia-induced inflammation, phagocytosis, and antigen presentation (62). In humans, increased microglial Kv1.3 expression has further been demonstrated in the postmortem brains of AD (25) and stroke (48) patients. Interestingly, the Kv1.3 blocker PAP-1 has been found to reduce neuroinflammation and improve cognition or neurological deficits in rodent models of AD and ischemic stroke (26, 48). However, Kv1.3-mediated current was reportedly reduced in striatal cholinergic neurons in a PD mouse model (63), similar to the finding that ion channel activity decreases

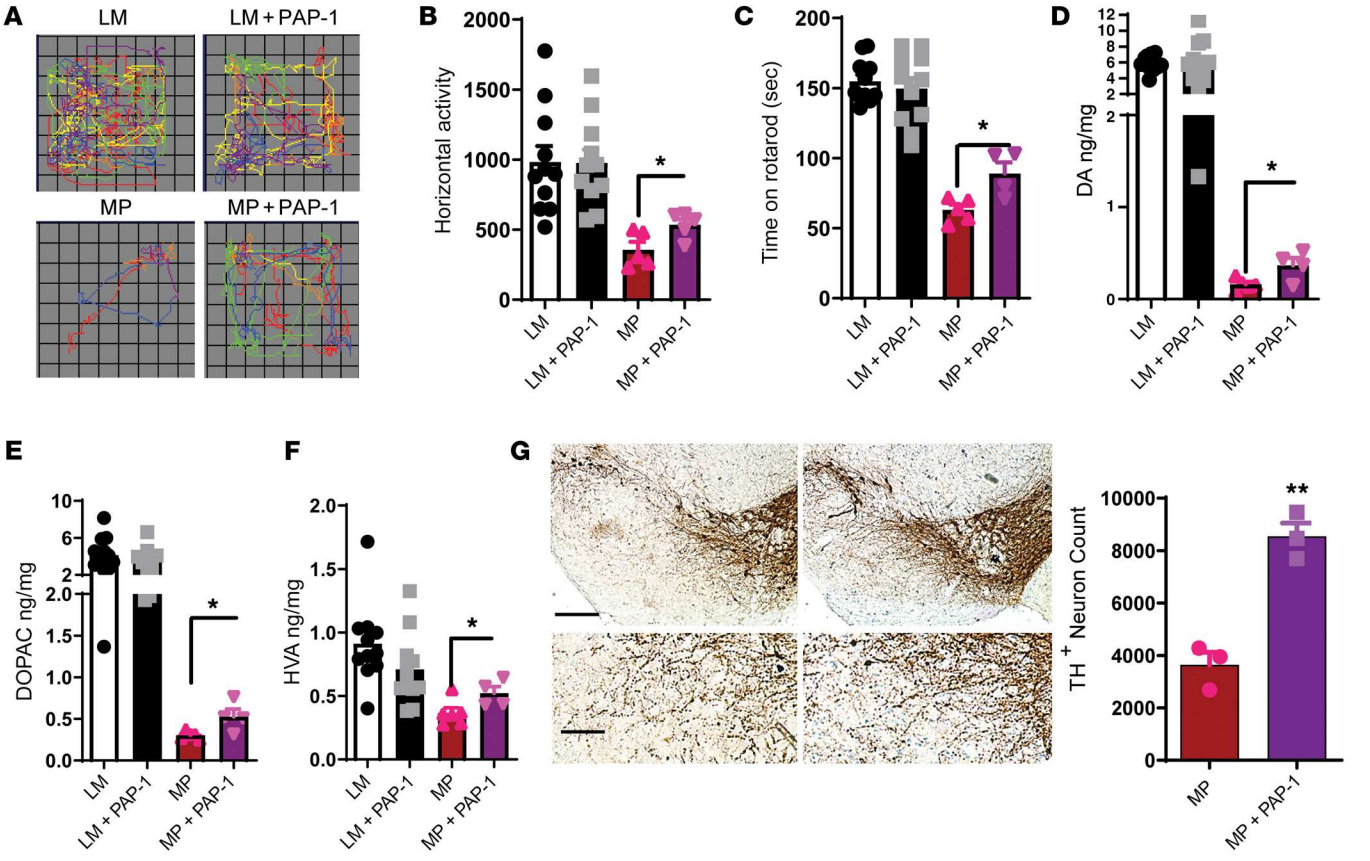
A
LM
LM + PAP-1
MP
MP + PAP-1
B
Horizontal activity
C
Time on rotarod (sec)
D
DA ng/mg
E
DOPAC ng/mg
F
HVA ng/mg
G
TH+ Neuron Count
H
Saline
MPTP
MPTP + PAP-1
I
Arbitrary units
Branches
Soma Size
J
Control
MPTP
MPTP + PAP-1
mRNA fold change
IL-1β
TNF-α
K
2x
10x
Saline
MPTP
MPTP + PAP-1
L
Number of TH+ neurons
Saline
MPTP
MPTP + PAP1

Figure 7. PAP-1 reduces inflammation and neurodegeneration in mouse models of PD. (**A**–**H**) MitoPark mouse model. (**A**) Representative movement tracks showing that PAP-1 rescued movement deficits of MitoPark mice at 20 weeks. (**B**) VersaMax open-field test showed increased horizontal activity of MitoPark mice treated with PAP-1 compared with the vehicle-treated control group. (**C**) Behavior test revealed increased time spent on the rotarod by MitoPark mice treated with PAP-1 compared with the vehicle-treated group. (**D**–**F**) HPLC showing that PAP-1 treatment protected MitoPark mice from loss of (**D**) dopamine (DA), (**E**) DOPAC, and (**F**) HVA. (**G**) IHC of SNpc showing that PAP-1 protected against loss of TH-positive neurons in MitoPark mice and stereology analysis of the SNpc showing that PAP-1 decreased the loss of TH-positive neurons in MitoPark mice. Scale bars: 200 μm (top panel); 100 μm (bottom panel). (**H**–**L**) MPTP mouse model. (**H**) IHC of MPTP-exposed substantia nigra and striatum showing that PAP-1 altered microgliosis. Scale bars: 50 μm (top panel); 20 μm (insets); 100 μm (bottom panel). (**I**) ImageJ analysis of MPTP-exposed substantia nigra showing that PAP-1 reduced soma size and increased the number of microglial branches. (**J**) qRT-PCR analysis of striatum after MPTP showing reduced mRNA expression of proinflammatory factors IL-1β and TNF-α. (**K**) IHC of SNpc showing that PAP-1 protected against MPTP-induced loss of TH-positive neurons. Scale bars: 500 μm (top panel); 200 μm (bottom panel). (**L**) Stereological analysis of the SNpc showing that PAP-1 decreased the loss of TH-positive neurons after MPTP treatment. One-way ANOVA was used to compare multiple groups. In most cases, Tukey's post hoc analysis was applied. Each dot on the bar graphs represents a biological replicate. Data are presented as the mean ± SEM, with 3–7 animals per group. $^{*}P \leq 0.05$, $^{**}P < 0.01$, and $^{***}P < 0.001$.

in dopaminergic neurons in animal models of PD (64). It is not clear how these findings of PD-dampened ion channel activity relate to the proof-of-concept animal studies reported here, which show that inhibition of microglial Kv1.3 with PAP-1 protected against neuronal loss and inflammation in PD models and which further support an important role for Kv1.3 in neuroinflammation.

The mechanistic underpinnings of Kv1.3 transcriptional regulation remain largely unknown. Recent Kv1.3 studies have implicated the enzyme cereblon in its epigenetic regulation (35), its age-dependent methylation in patients with colorectal cancer (65), and in DNA methylation of its promoter in breast cancer (66). Although p38 MAPK in microglia has been shown to modulate Kv1.3 expression in HIV glycoprotein 120–induced neurotoxicity (61), the proximal signaling node that upregulates Kv1.3 has yet to be defined. In this study, we demonstrated that the NF-κB and p38 MAPK pathways contribute to the αSyn_{Agg}-induced transcriptional upregulation of Kv1.3. Our group recently showed that Fyn is induced in cell culture and animal models of PD and is important in modulating microglial inflammation by mediating the NF-κB and p38 MAPK pathways (10, 27). Fyn inhibition has been shown to reduce neuroinflammation in AD (52). We also showed that Fyn is upstream of the proapoptotic and proinflammatory kinase PKCδ (27, 38). Fyn also has a role in regulating inflammation in AD, whereby inhibition of Fyn kinase with saracatinib was found to protect against neurodegeneration in rodent models of AD (52). We report here that Fyn and PKCδ regulate Kv1.3 transcription by regulating NF-κB and p38 MAPK signaling. We induced a significant reduction in Kv1.3 expression as well as in its transcriptional upregulation by pharmacologically inhibiting Fyn or genetically ablating Fyn expression. Collectively, our results identify, for the first time to our knowledge, the Fyn/PKCδ axis as a key upstream signaling node in modulating Kv1.3 transcriptional upregulation.

Posttranslational modification of potassium channels leading to modulation of channel activity has been actively researched. Kv1.3 has multiple phosphorylation sites, including both tyrosine and serine/threonine (39, 40). Jimenez-Perez et al. (67) implicated the tyrosine phosphorylation sites of Kv1.3 in modulating proliferation. Holmes et al. (39) demonstrated that endogenous kinases and phosphatases continuously phosphorylate and dephosphorylate Kv1.3 and that any change in this dynamic phosphorylation/dephosphorylation can drastically alter Kv1.3 activity. Various tyrosine kinase proteins, including v-Src, are known to phosphorylate Kv1.3, and different adaptor proteins, including Grb10, modulate this phosphorylation of Kv1.3, thereby differentially regulating its activity (21, 42). We show here that Fyn, a nonreceptor tyrosine kinase, can phosphorylate Kv1.3, thereby modulating its function. Though we have shown a direct interaction between Fyn and Kv1.3, our Kv1.3 Tyr135 mutant transfection study revealed a modest effect on inflammation. This may be due to other possible Fyn phosphorylation sites on Kv1.3. Further studies are required to fully understand the role of Fyn in modulating Kv1.3 activity.

Collectively, we demonstrate that Kv1.3 is upregulated in Parkinsonian models. This upregulation was proximally controlled by the Fyn/PKCδ kinase signaling cascade through the downstream mediator of the NF-κB and p38 MAPK pathways. Fyn could further phosphorylate Kv1.3, which modulated Kv1.3 channel activity. We show that Kv1.3 upregulation in PD models plays a major role in neuroinflammation-mediated neurodegeneration. These findings further demonstrate a probable Kv1.3-mediated signaling cascade (Supplemental Figure 10) that can modulate microglial inflammation in Parkinsonism. Our comprehensive preclinical evaluation of the Kv1.3 blocker PAP-1 in 3 different animal models of PD, including MitoPark transgenic, MPTP, and αSyn_{PFF} mouse models, provides credence to the translational relevance of Kv1.3 modulation in PD. The diverse roles of Kv1.3 emerging from our findings, together with other studies, reinforce the potential therapeutic implications of Kv1.3 modulators.

Methods

Further information can be found in Supplemental Methods.

Cell culture, primary culture, and treatments. Primary mouse microglia (PMCs) were isolated from mixed glial cultures using a magnetic bead separation protocol published previously by our laboratory (68, 69). The mixed glia cultures from P0 mouse pups from C57BL/6J mice were prepared. Primary cells were maintained in DMEM-F12 supplemented with 10% FBS, 1% sodium pyruvate, 1% glutamine, 1% penicillin-streptomycin, and 1% nonessential amino acids. An immortalized MMC line was donated by D.T. Golenbock (University of Massachusetts Medical School, Worcester, Massachusetts, USA). The MMC line was characterized by our group (45, 70–72) and Halle et al. (73) and cultured in DMEM medium containing 10% FBS, 1% glutamine, and 1% penicillin-streptomycin. Treatments were performed in 2% FBS-containing medium. GFP and human αSyn-overexpressing AAVs (AAV-GFP, 0.95×10^{13} viral particles/mL and AAV-SYN, 1×10^{13} viral particles/mL) were obtained from the University of North Carolina Viral Vector Core (Chapel Hill, North Carolina, USA). Both viral vectors were of the AAV-5 serotype and coded for GFP and human αSyn, respectively, under a chicken β-actin promoter.

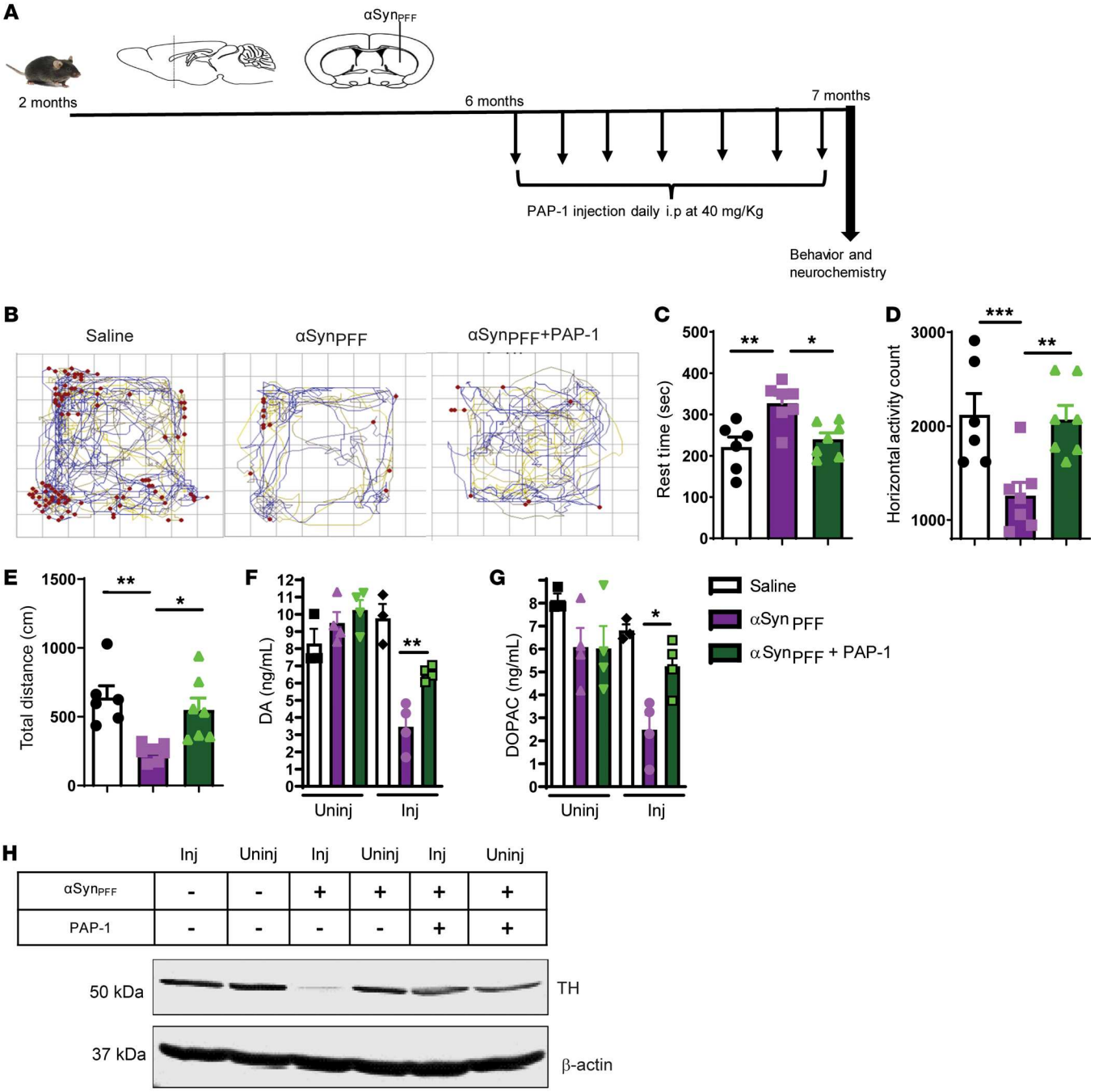

Figure 8. Kv1.3 inhibition protects against αSyn_{PFF}-induced behavior deficit and dopaminergic neuronal loss. (**A**) Treatment paradigm corresponding to the αSyn_{PFF} mouse model of PD. (**B**) Representative movement tracks showing that PAP-1 rescued movement deficits induced by αSyn_{PFF}. (**C**–**E**) A VersaMax open-field test showed decreased (**C**) rest time and increased (**D**) horizontal activity and (**E**) total distance traveled for αSyn_{PFF} mice treated with PAP-1. (**F** and **G**) HPLC showing that PAP-1 treatment protected against loss of (**F**) dopamine and (**G**) DOPAC induced by αSyn_{PFF}. (**H**) Western blot analysis of TH showing loss of TH induced by αSyn_{PFF} in the SNpc region. A 1-way ANOVA was used to compare multiple groups. In most cases, Tukey's post hoc analysis was applied. Each dot on the bar graphs represents a biological replicate. Data are presented as the mean ± SEM, with 3–7 animals per group. $^{*}P \leq 0.05$, $^{**}P < 0.01$, and $^{***}P < 0.001$.

Immortalized B cells from patients with PD and age-matched controls were obtained from the Coriell Institute for Medical Research (CIMR). Cell cultures of lymphoblasts obtained from the CIMR were maintained in RPMI 1640 media supplemented with 15% FBS, 2 mM L-glutamine, and 1% penicillin/streptomycin. The suspension cultures were kept in upright vented-cap T25 flasks with 10 mL media in incubators maintained at 37°C and 5% CO_2. Cells were initially seeded at 500,000 viable cells/mL and subcultured when they reached 1,000,000 viable cells/mL. Primary human microglial cells were a gift from Douglas Walker (Banner Sun Health Research Institute, Sun City, Arizona, USA).

Animal studies. All animals were housed under standard conditions of constant temperature (22 ± 1°C), humidity (relative, 30%), and a 12-hour light/12-hour dark cycle.

Human samples. SN tissues from patients with PD and age-matched controls were obtained from the Miami Brain Endowment Bank at the University of Miami (Miami, Florida, USA). The patients with PD were 82 ± 7.65 years of age ,and the unaffected controls were 80 ± 7.85 years of age. The samples were run and analyzed blindly.

Transfection study. The Kv1.3 WT and mutant plasmids were provided by Debra A. Fadool of Florida State University (Tallahassee, Florida, USA). For transfection, 250,000 MMCs were plated in 2 mL media per well on a 6-well plate. After 24 hours, cells were transfected with 3 μg plasmid DNA using Lipofectamine 2000 (Thermo Fisher Scientific) according to the manufacturer's protocol. The media were changed 12 hours after transfection and treated 48 hours after transfection.

Western blot analysis. Immunoblot analyses were performed following protocols described in our previously published studies (27, 38). Briefly, cells or tissues were homogenized and lysed using modified RIPA buffer. Proteins were normalized using a Bradford assay before loading onto a SDS-acrylamide gel. Protein (10–40 μg) was loaded into each well of 10%–18% acrylamide gels, which were run at 110 V for 2–3 hours at 4°C. Following separation, the proteins were transferred onto nitrocellulose membranes at 27 V for 18 hours at 4°C. After transfer, the membranes were blocked with LI-COR blocking buffer for 45 minutes and incubated in primary and then secondary antibodies following the manufacturer's protocol. The primary antibodies included anti-Kv1.3 (Alomone Labs, 1:1000) (Research Resource Identifier [RRID]: AB_2040151), anti-Kv1.3 (MilliporeSigma 1:1000) (RRID: AB_2265087), anti–p-p38 (Cell Signaling Technology, 1:1000) (RRID: AB_331641), anti-p38 (Cell Signaling Technology, 1:1000) (RRID: AB_330713), anti–p-Kv1.3 (MilliporeSigma, 1:1000, catalog SAB4504254), anti-PKCδ (Santa Cruz Biotechnology, 1:500) (RRID: AB_628145), anti-NLRP3 (AdipoGen, 1:1000) (RRID: AB_2490202), and anti–active MAPK (Promega, 1:2000). The secondary antibodies included IR-800–conjugated goat anti–mouse IgG (LI-COR, 1:20000) and IR-700–conjugated goat anti–rabbit IgG (LI-COR 1:20,000).

qRT-PCR. For RNA isolation, we followed previously published protocols (70, 74). Briefly, TRIzol Reagent (Thermo Fisher Scientific) was used to isolate total RNAs from cells or tissues. A NanoDrop spectrophotometer (Thermo Fisher Scientific) was used to quantify RNA, and 1 μg RNA was converted to cDNA using the High Capacity cDNA Synthesis Kit from Applied Biosystems (catalog 4368814). A quantitative SYBR Green PCR assay was performed using RT^2 qPCR SYBR Green Master Mix (Agilent Technologies) and prevalidated primers. The following validated primers from QIAGEN were used: pro–*IL-1β* (QT01048355), *Nos2* (QT00100275), *Mfn2* (QT00134295), *CSF2* (QT00251286), *IL-6* (QT00098875), *TNF-α* (QT00104006), mouse *Kv1.3* (QT00257467), human *Kv1.3* (QT00211197), *Kv1.1* (QT01537263), *Kv1.5* (QT00268387), *KCa3.1* (QT00105672), *Fyn* (QT00176666), and 18S rRNA (QT02448075). The primers for *MRC1* and *IRF4* were synthesized at ISU's DNA facility. The fold change in gene expression was determined by the ΔΔCt method, where Ct was the threshold value. 18S rRNA was used as the housekeeping gene.

IHC and ICC. IHC was performed on 30-μm mouse striatal and nigral sections as well as human nigral sections as described in our previous publications (75, 76). For antigen retrieval, 10 mM citrate buffer at pH 7.4 was used for animal samples, whereas citraconic anhydride was used for human samples. Following antigen retrieval, sections were washed with PBS, blocked with blocking buffer (2% BSA, 0.5% Triton X-100, and 0.05% Tween-20), and incubated in primary antibodies overnight at 4°C. Next, sections were washed with PBS, incubated in secondary antibodies for 1 hour, and stained with Hoechst nuclear dye. Finally, sections were mounted on precoated slides and dried overnight before visualization under a fluorescence microscope. Confocal imaging was performed on these sections at ISU's Microscope Facility using a Leica DMIRE2 confocal microscope with a ×63 oil objective. For *Z*-stacking, each optical section consisted of ten to fifteen 0.5-μm-thick slices.

For ICC on immortalized MMCs and PMCs, 4% paraformaldehyde (PFA) was used to fix the cells. Next, fixed cells were washed with PBS, blocked using a blocking buffer, and incubated in primary antibodies following the manufacturer's protocol. Following overnight primary antibody incubation, cells were washed with PBS, incubated in secondary antibodies for 75 minutes, and mounted onto slides using Fluoromount Aqueous Mounting Medium (MilliporeSigma). Samples were visualized using an inverted fluorescence microscope (TE-2000U, Nikon). For DAB staining, we followed previously published protocols from our laboratory (27, 38, 77). The following primary antibodies were used: IBA1 (Wako, 1:1000) (RRID: AB_2314667), IBA1 (Abcam, 1:500) (RRID: AB_870576), Kv1.3 (Alomone Labs, 1:500) (RRID: AB_2040151), Kv1.3 (MilliporeSigma, 1:500)(RRID: AB_11212692), p-Kv1.3 (MilliporeSigma 1:500) (SAB4504254), p38 (Cell Signaling Technology, 1:500) (RRID: AB_330713), and tyrosine hydroxylase (TH) (MilliporeSigma, 1:1000) (RRID: AB_2201526). Alexa dye–conjugated secondary antibodies were used for both ICC and IHC.

Flow cytometry. MMCs (50,000/well) were plated onto 12-well cell culture plates. Cells were treated with 1 μg/mL LPS or 1 μM αSyn_{Agg} for 24 hours. Following treatment, cells were double washed with HBSS and blocked with 2% BSA in HBSS for 30 minutes at 37°C. After blocking, cells were incubated in the Kv1.3 antibody conjugated to FITC (1:1000, in 1% BSA in HBSS) (RRID: AB_2040147) for 1 hour at 37°C. Following incubation, any unbound antibody was double washed with HBSS, and the cells were scraped from the plate and suspended in 500 μL HBSS. A FACSCanto Cell Analyzer (BD Biosciences) was used for flow cytometric analysis at ISU's flow cytometry facility.

Duolink PLA. Duolink PLA was performed according to previously published methods (78). Briefly, 10,000 PMCs/well were plated on coverslips in 96-well cell culture plates. Cells were treated with 1 μM αSyn_{Agg} for 24 hours, after which the cells were fixed with 4% PFA, blocked (2% BSA, 0.5% Triton X-100, 0.05% Tween-20 in PBS), and incubated overnight in primary antibody solutions. Following primary antibody incubation, a Duolink In Situ Red Starter Kit (MilliporeSigma; DUO92101) was used according to the manufacturer's protocol. A mouse Fyn monoclonal antibody (Thermo Fisher Scientific, 1:500) (RRID: AB_1074491) and a rabbit Kv1.3 antibody (Alomone Labs, 1:500) (RRID: AB_2040151) were used as primary antibodies. Slides were imaged using a Leica DMIRE2 confocal microscope with a ×63 oil objective. For *Z*-stacking, each optical section consisted of ten to fifteen 0.5-μm-thick slices.

Immunoprecipitation. Immunoprecipitation was performed following our laboratory's previously published protocol (27). Briefly, 5×10^6 microglial cells were homogenized using NP40 lysis buffer. Lysates were incubated overnight with the Fyn antibody (Thermo Fisher Scientific, RRID: AB_1074491) and the Kv1.3 antibody (Alomone Labs, RRID: AB_2040151) separately. Protein G–sepharose

beads were used for pulldown. The lysates were incubated with the protein G–sepharose beads and then washed 4 times before loading.

Whole-cell patch clamping. PMCs were plated at 100,000–150,000 cells per well in 24-well plates for 8–12 hours before stimulation with either 300 ng/mL LPS or 1 μM αSyn_{Agg} in the presence or absence of 10 μM saracatinib. After a 40- to 48-hour stimulation, cells were detached by trypsinization, washed, attached to poly-L-lysine–coated glass coverslips, and then studied within 20–90 minutes after plating in the whole-cell mode of the patch-clamp technique with an EPC-10 HEKA amplifier (HEKA Elektronik). B lymphocytes were thawed, plated, and maintained in a tissue culture incubator for 30–60 minutes before recording. All currents were recorded in normal Ringer's solution containing 160 mM NaCl, 4.5 mM KCl, 2 mM $CaCl_2$, 1 mM $MgCl_2$, and 10 mM HEPES (adjusted to pH 7.4 and 290–310 mOsm). Patch pipettes were pulled from soda-lime glass (micro-hematocrit tubes, Kimble Chase) to resistances of 2–3 MΩ when submerged in the bath solution and filled with a KF-based Ca^{2+}-free internal pipette solution containing 145 mM KF, 2 mM $MgCl_2$, 10 mM HEPES, and 10 mM EGTA (pH 7.2, 290–310 mOsm). On the basis of our previous publication identifying Kir2.1, Kv1.3 and KCa3.1 as the major K^+ channels expressed in cultured microglia (21), recording conditions were set up to isolate Kv1.3 currents. The use of KF avoids "contaminating" Kv currents by calcium-activated K^+ currents or chloride currents. Currents were elicited with a "use-dependence protocol," involving a train of ten 200-ms voltage steps from –80 to 40 mV applied at a frequency of 1 Hz, which identifies Kv1.3 by its characteristic use dependence (e.g., current amplitude declines rapidly when pulsed faster than the channels can recover from inactivation). In 25% of the cells, we then further pharmacologically confirmed that the current was predominantly carried by Kv1.3 by testing its sensitivity to PAP-1. Cell capacitance, which directly measures the cell-surface area, and access resistance were continuously monitored during recordings. Kv1.3 current density was calculated as the use-dependent current amplitude at 40 mV divided by the cell capacitance measured for individual cells.

HPLC. HPLC for neurotransmitters was performed following previously published methods (70). Briefly, the left mouse striatum was weighed and lysed using an extraction solution (0.1 M perchloric acid containing 0.05% Na_2 EDTA and 0.1% $Na_2S_2O_5$) and isoproterenol (internal standard). A C-18 reversed-phase column isocratically separated dopamine, 3,4-dihydroxyphenylacetic acid (DOPAC), homovanillic acid (HVA), and norepinephrine (NE) using a Dionex Ultimate 3000 HPLC system (pump ISO-3100SD, Thermo Scientific) attached to an electrochemical detection system consisting of the CoulArray Model 5600A (Thermo Fisher Scientific) coupled with an analytical cell (microdialysis cell 5014B) and a guard cell (model 5020) with the 4-channel potentials set at 350, 0, –150, and 220 mV. Chromeleon 7 and ESA CoulArray 3.10 HPLC software were used for data acquisition and analysis.

Multiplex cytokine assay. Multiple cytokine assays were performed according to our previous publication (27). Briefly, 40 μL treatment media were incubated overnight with 40 μL primary antibodies conjugated with magnetic beads. Following incubation with primary antibodies, the samples were washed, incubated with biotinylated antibody and biotin/streptavidin, and then assayed on a Bio-Plex plate reader (Bio-Rad). Standards were obtained from PeproTech.

Griess assay. Griess assays were performed as we previously described (27). Briefly, after treatment, 50 μL medium was incubated with 50 μL Griess reagent for 10 minutes, and a plate reader was used to read the absorbance at 540 nm.

Statistics. GraphPad 5.0 was used for statistical analysis, with *P* values of 0.05 or less considered statistically significant. One-way ANOVA was used for comparing multiple groups. In most cases, Tukey's post hoc analysis was applied. A 2-tailed Student's *t* test was used when comparing 2 groups.

Study approval. The laboratory animal facility of ISU is fully accredited by the Association for Assessment and Accreditation of Laboratory Animal Care (AAALAC), and all procedures involving animal handling were approved by the IACUC at ISU. Human brain samples were obtained from the brain repositories of the UCD Alzheimer's Disease Center (P30 AG10129) with IRB approval.

Author contributions

SS, AGK, and HW conceived the study. SS, DR, VS, HMN, JL, EM, and MG developed methodology. SS, DR, VS, HMN, JL, EM, ML, BNP, NS, SM, MN, MG, AA, PA, NP, VS, MA, AC, DH, LWJ, SR, HW, and AGK performed experiments and analyses. SS, HJ, VA, AGK, and HW wrote the original draft of the manuscript. SS, AGK, HJ, SR, VA, HW, and HMN reviewed and edited the manuscript. AGK and HW acquired funding. AGK, HW, SR, and LWJ provided resources.

Acknowledgments

This study was supported by NIH grant NS100090. Experimental supplies and salaries were also partially supported by other NIH grants (ES026892 and NS088206). This work was also supported in part by NIH grants P30 AG10129 and 1K08NS099474-01 (to SR) to supply AD and DLB samples. We give special thanks to Douglas T. Golenbock of the University of Massachusetts Medical School for providing the MMC cell line and Debra A. Fadool of Florida State University for providing the Kv.1.3 and mutant plasmids. We also acknowledge the Lloyd Endowed Chair and Eminent Scholar and the Armbrust endowment to AGK. We also thank Gary Zenitsky for assistance in preparing this manuscript.

Address correspondence to: Anumantha Kanthasamy, Department of Biomedical Sciences, Iowa State University, Ames, Iowa 50011, USA. Phone: 515.294.2516; Email: akanthas@iastate.edu

SS's present affiliation is: Department of Pathology, Brigham and Women's Hospital, Harvard Medical School, Boston, Massachusetts, USA.

MA's present affiliation is: Department of Genetics and Bioengineering, Alanya Alaaddin Keykubat University, Antalya, Turkey.

1. Doorn KJ, et al. Emerging roles of microglial activation and non-motor symptoms in Parkinson's disease. *Prog Neurobiol*. 2012;98(2):222–238.
2. Wolters ECh. Non-motor extranigral signs and symptoms in Parkinson's disease. *Parkinsonism Relat Disord*. 2009;15 Suppl 3:S6–12.
3. Tansey MG, Goldberg MS. Neuroinflammation in Parkinson's disease: its role in neuronal death and implications for therapeutic intervention. *Neurobiol Dis*. 2010;37(3):510–518.
4. Block ML, Zecca L, Hong JS. Microglia-mediated neurotoxicity: uncovering the molecular mecha-

nisms. *Nat Rev Neurosci*. 2007;8(1):57–69.
5. Glass CK, Saijo K, Winner B, Marchetto MC, Gage FH. Mechanisms underlying inflammation in neurodegeneration. *Cell*. 2010;140(6):918–934.
6. Imamura K, Hishikawa N, Sawada M, Nagatsu T, Yoshida M, Hashizume Y. Distribution of major histocompatibility complex class II-positive microglia and cytokine profile of Parkinson's disease brains. *Acta Neuropathol*. 2003;106(6):518–526.
7. Kim C, et al. Neuron-released oligomeric α-synuclein is an endogenous agonist of TLR2 for paracrine activation of microglia. *Nat Commun*. 2013;4:1562.
8. Gustot A, Gallea JI, Sarroukh R, Celej MS, Ruysschaert JM, Raussens V. Amyloid fibrils are the molecular trigger of inflammation in Parkinson's disease. *Biochem J*. 2015;471(3):323–333.
9. Codolo G, et al. Triggering of inflammasome by aggregated α-synuclein, an inflammatory response in synucleinopathies. *PLoS ONE*. 2013;8(1):e55375.
10. Panicker N, et al. Fyn kinase regulates misfolded α-synuclein uptake and NLRP3 inflammasome activation in microglia. *J Exp Med*. 2019;216(6):1411–1430.
11. Daniele SG, Béraud D, Davenport C, Cheng K, Yin H, Maguire-Zeiss KA. Activation of MyD88-dependent TLR1/2 signaling by misfolded α-synuclein, a protein linked to neurodegenerative disorders. *Sci Signal*. 2015;8(376):ra45.
12. Lee EJ, et al. Alpha-synuclein activates microglia by inducing the expressions of matrix metalloproteinases and the subsequent activation of protease-activated receptor-1. *J Immunol*. 2010;185(1):615–623.
13. Chandy KG, et al. A family of three mouse potassium channel genes with intronless coding regions. *Science*. 1990;247(4945):973–975.
14. Swanson R, et al. Cloning and expression of cDNA and genomic clones encoding three delayed rectifier potassium channels in rat brain. *Neuron*. 1990;4(6):929–939.
15. Matteson DR, Deutsch C. K channels in T lymphocytes: a patch clamp study using monoclonal antibody adhesion. *Nature*. 1984;307(5950):468–471.
16. DeCoursey TE, Chandy KG, Gupta S, Cahalan MD. Voltage-gated K^+ channels in human T lymphocytes: a role in mitogenesis? *Nature*. 1984;307(5950):465–468.
17. Koschak A, Bugianesi RM, Mitterdorfer J, Kaczorowski GJ, Garcia ML, Knaus HG. Subunit composition of brain voltage-gated potassium channels determined by hongotoxin-1, a novel peptide derived from *Centruroides limbatus* venom. *J Biol Chem*. 1998;273(5):2639–2644.
18. Xu J, et al. The voltage-gated potassium channel Kv1.3 regulates peripheral insulin sensitivity. *Proc Natl Acad Sci USA*. 2004;101(9):3112–3117.
19. Upadhyay SK, et al. Selective Kv1.3 channel blocker as therapeutic for obesity and insulin resistance. *Proc Natl Acad Sci USA*. 2013;110(24):E2239–E2248.
20. Gocke AR, et al. Kv1.3 deletion biases T cells toward an immunoregulatory phenotype and renders mice resistant to autoimmune encephalomyelitis. *J Immunol*. 2012;188(12):5877–5886.
21. Fadool DA, et al. Kv1.3 channel gene-targeted deletion produces "Super-Smeller Mice" with altered glomeruli, interacting scaffolding proteins, and biophysics. *Neuron*. 2004;41(3):389–404.
22. Fordyce CB, Jagasia R, Zhu X, Schlichter LC. Microglia Kv1.3 channels contribute to their ability to kill neurons. *J Neurosci*. 2005;25(31):7139–7149.
23. Nguyen HM, et al. Differential Kv1.3, KCa3.1, and Kir2.1 expression in "classically" and "alternatively" activated microglia. *Glia*. 2017;65(1):106–121.
24. Di Lucente J, Nguyen HM, Wulff H, Jin LW, Maezawa I. The voltage-gated potassium channel Kv1.3 is required for microglial pro-inflammatory activation in vivo. *Glia*. 2018;66(9):1881–1895.
25. Rangaraju S, Gearing M, Jin LW, Levey A. Potassium channel Kv1.3 is highly expressed by microglia in human Alzheimer's disease. *J Alzheimers Dis*. 2015;44(3):797–808.
26. Maezawa I, et al. Kv1.3 inhibition as a potential microglia-targeted therapy for Alzheimer's disease: preclinical proof of concept. *Brain*. 2018;141(2):596–612.
27. Panicker N, et al. Fyn kinase regulates microglial neuroinflammatory responses in cell culture and animal models of Parkinson's disease. *J Neurosci*. 2015;35(27):10058–10077.
28. Schmitz A, et al. Design of PAP-1, a selective small molecule Kv1.3 blocker, for the suppression of effector memory T cells in autoimmune diseases. *Mol Pharmacol*. 2005;68(5):1254–1270.
29. Alvarez-Erviti L, Couch Y, Richardson J, Cooper JM, Wood MJ. Alpha-synuclein release by neurons activates the inflammatory response in a microglial cell line. *Neurosci Res*. 2011;69(4):337–342.
30. Khodr CE, et al. An α-synuclein AAV gene silencing vector ameliorates a behavioral deficit in a rat model of Parkinson's disease, but displays toxicity in dopamine neurons. *Brain Res*. 2011;1395:94–107.
31. Ekstrand MI, et al. Progressive parkinsonism in mice with respiratory-chain-deficient dopamine neurons. *Proc Natl Acad Sci USA*. 2007;104(4):1325–1330.
32. Gordon R, et al. Inflammasome inhibition prevents α-synuclein pathology and dopaminergic neurodegeneration in mice. *Sci Transl Med*. 2018;10(465):eaah4066.
33. Vila M, Vukosavic S, Jackson-Lewis V, Neystat M, Jakowec M, Przedborski S. Alpha-synuclein up-regulation in substantia nigra dopaminergic neurons following administration of the parkinsonian toxin MPTP. *J Neurochem*. 2000;74(2):721–729.
34. Kowall NW, Hantraye P, Brouillet E, Beal MF, McKee AC, Ferrante RJ. MPTP induces alpha-synuclein aggregation in the substantia nigra of baboons. *Neuroreport*. 2000;11(1):211–213.
35. Kang JA, et al. Epigenetic regulation of Kcna3-encoding Kv1.3 potassium channel by cereblon contributes to regulation of $CD4^+$ T-cell activation. *Proc Natl Acad Sci USA*. 2016;113(31):8771–8776.
36. D'Addario M, Arora PD, McCulloch CA. Role of p38 in stress activation of Sp1. *Gene*. 2006;379:51–61.
37. Saha RN, Jana M, Pahan K. MAPK p38 regulates transcriptional activity of NF-kappaB in primary human astrocytes via acetylation of p65. *J Immunol*. 2007;179(10):7101–7109.
38. Gordon R, et al. Protein kinase Cδ upregulation in microglia drives neuroinflammatory responses and dopaminergic neurodegeneration in experimental models of Parkinson's disease. *Neurobiol Dis*. 2016;93:96–114.
39. Holmes TC, Fadool DA, Levitan IB. Tyrosine phosphorylation of the Kv1.3 potassium channel. *J Neurosci*. 1996;16(5):1581–1590.
40. Bowlby MR, Fadool DA, Holmes TC, Levitan IB. Modulation of the Kv1.3 potassium channel by receptor tyrosine kinases. *J Gen Physiol*. 1997;110(5):601–610.
41. Chung I, Schlichter LC. Regulation of native Kv1.3 channels by cAMP-dependent protein phosphorylation. *Am J Physiol*. 1997;273(2 Pt 1):C622–C633.
42. Cook KK, Fadool DA. Two adaptor proteins differentially modulate the phosphorylation and biophysics of Kv1.3 ion channel by SRC kinase. *J Biol Chem*. 2002;277(15):13268–13280.
43. Yamada E, Bastie CC. Disruption of Fyn SH3 domain interaction with a proline-rich motif in liver kinase B1 results in activation of AMP-activated protein kinase. *PLoS ONE*. 2014;9(2):e89604.
44. Notredame C, Higgins DG, Heringa J. T-Coffee: a novel method for fast and accurate multiple sequence alignment. *J Mol Biol*. 2000;302(1):205–217.
45. Sarkar S, et al. Characterization and comparative analysis of a new mouse microglial cell model for studying neuroinflammatory mechanisms during neurotoxic insults. *Neurotoxicology*. 2018;67:129–140.
46. Kundu-Raychaudhuri S, Chen YJ, Wulff H, Raychaudhuri SP. Kv1.3 in psoriatic disease: PAP-1, a small molecule inhibitor of Kv1.3 is effective in the SCID mouse psoriasis--xenograft model. *J Autoimmun*. 2014;55:63–72.
47. Beeton C, et al. Kv1.3 channels are a therapeutic target for T cell-mediated autoimmune diseases. *Proc Natl Acad Sci USA*. 2006;103(46):17414–17419.
48. Chen YJ, Nguyen HM, Maezawa I, Jin LW, Wulff H. Inhibition of the potassium channel Kv1.3 reduces infarction and inflammation in ischemic stroke. *Ann Clin Transl Neurol*. 2018;5(2):147–161.
49. Pereira LE, Villinger F, Wulff H, Sankaranarayanan A, Raman G, Ansari AA. Pharmacokinetics, toxicity, and functional studies of the selective Kv1.3 channel blocker 5-(4-phenoxybutoxy)psoralen in rhesus macaques. *Exp Biol Med (Maywood)*. 2007;232(10):1338–1354.
50. Morrison HW, Filosa JA. A quantitative spatiotemporal analysis of microglia morphology during ischemic stroke and reperfusion. *J Neuroinflammation*. 2013;10:4.
51. Karuppagounder SS, Brahmachari S, Lee Y, Dawson VL, Dawson TM, Ko HS. The c-Abl inhibitor, nilotinib, protects dopaminergic neurons in a preclinical animal model of Parkinson's disease. *Sci Rep*. 2014;4:4874.
52. Nygaard HB, van Dyck CH, Strittmatter SM. Fyn kinase inhibition as a novel therapy for Alzheimer's disease. *Alzheimers Res Ther*. 2014;6(1):8.
53. McGeer PL, Itagaki S, Boyes BE, McGeer EG. Reactive microglia are positive for HLA-DR in the substantia nigra of Parkinson's and Alzheimer's disease brains. *Neurology*. 1988;38(8):1285–1291.
54. Perry VH. Innate inflammation in Parkinson's disease. *Cold Spring Harb Perspect Med*.

2012;2(9):a009373.
55. Mao X, et al. Pathological α-synuclein transmission initiated by binding lymphocyte-activation gene 3. *Science*. 2016;353(6307):aah3374.
56. Harischandra DS, et al. Manganese promotes the aggregation and prion-like cell-to-cell exosomal transmission of α-synuclein. *Sci Signal*. 2019;12(572):eaau4543.
57. Chimote AA, Kuras Z, Conforti L. Disruption of kv1.3 channel forward vesicular trafficking by hypoxia in human T lymphocytes. *J Biol Chem*. 2012;287(3):2055–2067.
58. Li H, Lemay S, Aoudjit L, Kawachi H, Takano T. SRC-family kinase Fyn phosphorylates the cytoplasmic domain of nephrin and modulates its interaction with podocin. *J Am Soc Nephrol*. 2004;15(12):3006–3015.
59. Cahalan MD, Chandy KG. The functional network of ion channels in T lymphocytes. *Immunol Rev*. 2009;231(1):59–87.
60. Wang T, et al. Activated T-cells inhibit neurogenesis by releasing granzyme B: rescue by Kv1.3 blockers. *J Neurosci*. 2010;30(14):5020–5027.
61. Liu J, Xu C, Chen L, Xu P, Xiong H. Involvement of Kv1.3 and p38 MAPK signaling in HIV-1 glycoprotein 120-induced microglia neurotoxicity. *Cell Death Dis*. 2012;3:e254.
62. Rangaraju S, et al. A systems pharmacology-based approach to identify novel Kv1.3 channel-dependent mechanisms in microglial activation. *J Neuroinflammation*. 2017;14(1):128.
63. Tubert C, et al. Decrease of a current mediated by Kv1.3 channels causes striatal cholinergic interneuron hyperexcitability in experimental Parkinsonism. *Cell Rep*. 2016;16(10):2749–2762.
64. Branch SY, Chen C, Sharma R, Lechleiter JD, Li S, Beckstead MJ. Dopaminergic neurons exhibit an age-dependent decline in electrophysiological parameters in the MitoPark mouse model of Parkinson's disease. *J Neurosci*. 2016;36(14):4026–4037.
65. He T, et al. Epigenetic regulation of voltage-gated potassium ion channel molecule Kv1.3 in mechanisms of colorectal cancer. *Discov Med*. 2017;23(126):155–162.
66. Brevet M, Haren N, Sevestre H, Merviel P, Ouadid-Ahidouch H. DNA methylation of K(v)1.3 potassium channel gene promoter is associated with poorly differentiated breast adenocarcinoma. *Cell Physiol Biochem*. 2009;24(1-2):25–32.
67. Jiménez-Pérez L, et al. Molecular determinants of Kv1.3 potassium channels-induced proliferation. *J Biol Chem*. 2016;291(7):3569–3580.
68. Gordon R, Hogan CE, Neal ML, Anantharam V, Kanthasamy AG, Kanthasamy A. A simple magnetic separation method for high-yield isolation of pure primary microglia. *J Neurosci Methods*. 2011;194(2):287–296.
69. Sarkar S, et al. Rapid and refined CD11b magnetic isolation of primary microglia with enhanced purity and versatility. *J Vis Exp*. 2017;(122):55364.
70. Sarkar S, et al. Manganese exposure induces neuroinflammation by impairing mitochondrial dynamics in astrocytes. *Neurotoxicology*. 2018;64:204–218.
71. Sarkar S, et al. Manganese activates NLRP3 inflammasome signaling and propagates exosomal release of ASC in microglial cells. *Sci Signal*. 2019;12(563):eaat9900.
72. Sarkar S, et al. Molecular Signatures of neuroinflammation induced by αSynuclein aggregates in microglial cells. *Front Immunol*. 2020;11:33.
73. Halle A, et al. The NALP3 inflammasome is involved in the innate immune response to amyloid-beta. *Nat Immunol*. 2008;9(8):857–865.
74. Seo J, Ottesen EW, Singh RN. Antisense methods to modulate pre-mRNA splicing. *Methods Mol Biol*. 2014;1126:271–283.
75. Ghosh A, et al. Mitoapocynin treatment protects against neuroinflammation and dopaminergic neurodegeneration in a preclinical animal model of Parkinson's disease. *J Neuroimmune Pharmacol*. 2016;11(2):259–278.
76. Ghosh A, et al. Anti-inflammatory and neuroprotective effects of an orally active apocynin derivative in pre-clinical models of Parkinson's disease. *J Neuroinflammation*. 2012;9:241.
77. Langley M, et al. Mito-Apocynin Prevents Mitochondrial Dysfunction, Microglial Activation, Oxidative Damage, and Progressive Neurodegeneration in MitoPark Transgenic Mice. *Antioxid Redox Signal*. 2017;27(14):1048–1066.
78. Sarkar S, et al. Mitochondrial impairment in microglia amplifies NLRP3 inflammasome proinflammatory signaling in cell culture and animal models of Parkinson's disease. *NPJ Parkinsons Dis*. 2017;3:30.